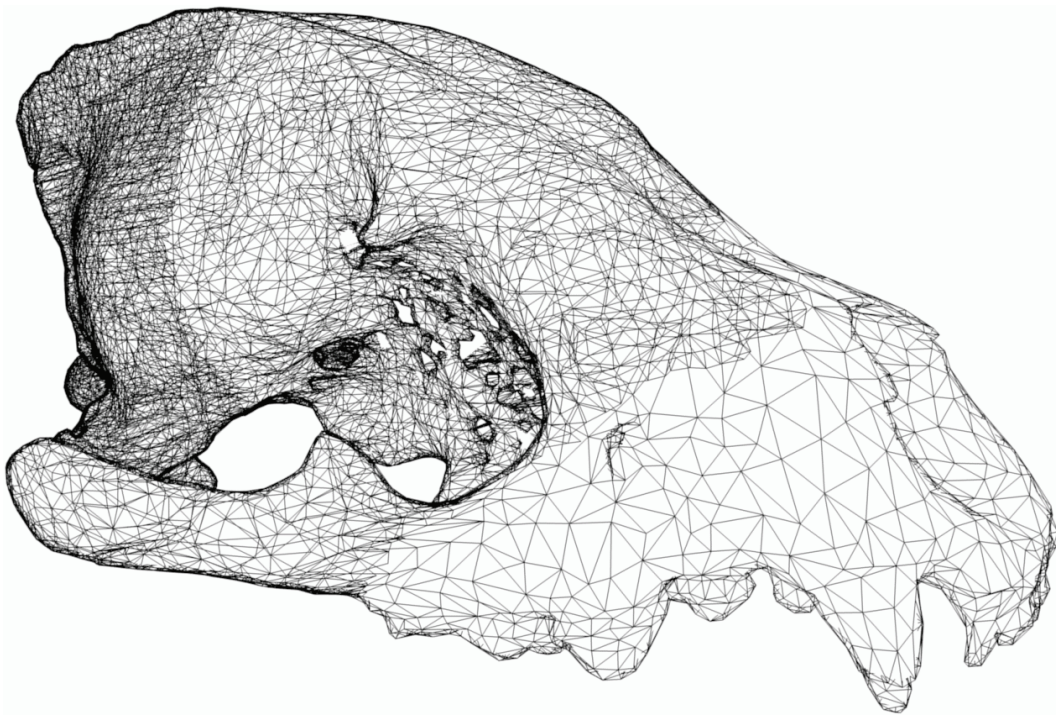# Comparison of *Crocuta crocuta crocuta* and *Crocuta crocuta spelaea* through computer tomography

Martin Dockner

Comparison of *Crocuta crocuta crocuta* and *Crocuta crocuta spelaea* through computer tomography

Martin Dockner

December 22, 2006

A Thesis Submitted to the Graduate Faculty of Geosciences, Geography and Astronomy in Partial Fulfillment of the Requirements for the Degree of Master of Science, written at the Department of Paleontology, University of Vienna

dedicated to my father
Leopold Dockner

Contents

Abstract

Long used in medical investigation, computer tomography is a new technique in palaeontology. The strength of this non-destructive visualisation method lies in the exact three-dimensional x-rays which can be further processed on the computer. As the visualisation is made of voxels (= three dimensional pixels) with known volume and side-length, it is possible to measure exact length, face or volume of an abstract body. These advantages enable this study to present a picture of the nearly inaccessible cranial cavities of hyaenid skulls. The main interest was centered on the sinal cavities which represent a special skull trait in hyaenine hyaenids compared to other carnivores. Through use of computer tomography volume data could be acquired about the endocranial and the sinal cavities of the analysed specimens. The special feature of these sinal cavities are their enormous size which is rare in carnivores.[1]

This study tries to find coherences between sinal cavities, cranial capacity and skull size, as well as the verification or negation of the theoretical sinal cavitiy size difference in recent and extinct hyaenids. Until now the proposed size of sinal cavities in fossil cave hyenas was believed to be much larger than in recent hyenas. This was in connection with ecological differences and behaviour.

The analysis of fossil and recent hyaenid specimens however shows clearly that there is no typical difference in sinus-size which can be used for taxonomic reasons. The size differences are so undifferentiated, that no coherence can be found. On the other hand, cranial capacity (and thus brain size) shows a typical behaviour in expanding with growing skull size.

---

[1]The only exception is the cave bear *Ursus spelaeus* and its close relatives.

1 Introduction

The cave hyena *Crocuta crocuta spelaea* is quite common in European caves. Its fossil record—even if not nearly as rich as that of the cave bear—has led to common theories about its life and habitat in glacial Europe. Different systematic characteristics were used for comparison of these fossil hyenas with recent living hyenas in Africa and Asia. Some of these studies produced good results, using both cranial and post-cranial features. One special trait was discovered in living hyaenids even before the analysis of fossil material. In all of the recent hyaenine hyaenids (which comprise of *Crocuta crocuta crocuta*,*Hyaena hyaena* and *Parahyaena brunnea*[1]) there are very large developed nasal sinuses overlapping the cranial region of the skull.

The nasal sinus cavities are common in every land living mammal to a greater or lesser extent. In carnivores the frontal sinus is normally well developed but thins out in the dorsal area. The sinal cavities of carnivores normally overlap the endocranium by about one third. In hyaenine hyaenids the dorsal part of the sinal cavities reaches far over the endocranium, sometimes overlapping it completely. The background of this unique feature is not known, though some more or less plausible theories exist.

The same vaulting of the skull can be found in fossil specimens of *Crocuta crocuta spelaea*. The development of the cavities is similar to recent hyenas, but some small differences are visible with the unaided eye. Upon this a theory was built to compare the sinal cavities in fossil and recent material in search of another taxonomic or systematic feature.

The main problem for a long time was the impossibility of measuring these cavities in any rational way. Unlike the endocranial cavity which is well accessible through the foramen magnum, the sinal cavities lack such a simple access route. For a long time the only way to acquire data about these traits was using roentgen technology or breaking open the skull to get access to it. While x-rays where at least useful to measure distances, the three-dimensional features of the nasal sinuses where completely lost. Cutting a skull open to get direct access to the cavities was, on the other hand, not an option for precious fossil specimens, and thus also an unavailable method.

With the invention of computer tomography in the late 1970's a new possibility was opened up for acquiring data about these unusual skull-traits. With CT-technology it was possible for the first time to make exact three-dimensional doubles of the scanned object without damaging it. Especially scanning inanimate objects, like the different specimens in this study, yields very good results for further research.

---

[1]There is a fourth living hyaenid today, which is not a hyaenine hyaenid. *Proteles cristatus* is, due to special evolutionary tendencies in its diet, a member of the subfamily of proteline hyaenids.

The five specimens of *Crocuta crocuta spelaea* used for this study are from different excavation sites in Europe. Even if the cave hyena is actually quite common in European caves, the fossils are often limited to single bones, teeth or even only feeding traces on other animal bones. A complete skull, especially with the interior intact for examination as it was in this study, is really very precious and rare. To illustrate how common the cave hyena was in Europe in the Quaternary, the map in figure 1.1 shows the distribution of *Crocuta crocuta spelaea* in European caves after Musil (1980, 1981), Jánossy (1986) and Stuart (1991).
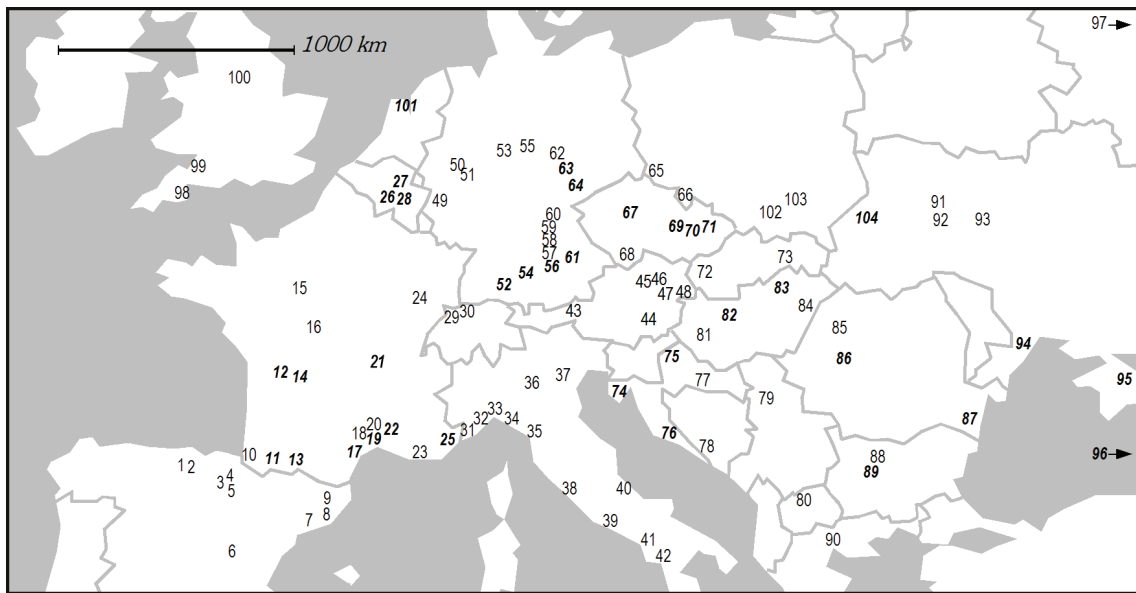
Figure 1.1: Distribution of *Crocuta crocuta spelaea* in West- and Central Europe in the Quaternary based on fossil findings in cave excavation sites. Bold and italic numbers indicate compilations of caves in close proximity to each other. 1 Castillo; 2 Otero; 3 Lezetxiki; 4 Aizkirri-Ko-Kobea; 5 Coseobilo; 6 Los Casares; 7 Abri Romani; 8 Toll; 9 Mollet; 10 Isturitz; *11* Beaudéance, d'Aurensan, Gerde, La Bouhadère, L'oeil, Montmaurin; *12* Fontéchevade, Rois; *13* Ariègeoise, Gargas; *14* Bernous, Jaurens, La Ferrassie; 15 Paris; 16 Pair-non-Pair; *17* Aldene, Crouzade, Tournal; 18 Roquette II; *19* Balauzière, Baume Fladin, Baume Longue, Calmette, Campefiel, Mialet; 20 Neron à Soyons; *21* Renne, Tasnières; *22* Fournier, Goule, Vallescure; 23 Rigabe; 24 Echenoz; *25* Cavillon, Enfants, Grimaldi, Observatoire, Prince; *26* Hyène, Surean, Èrable, Margite; *27* Grand abri Ben-Ahin, Dubois, Mont Falise, du Renard; *28* Hastière, La Naulette, Ramioul; 29 Liesbergmühle; 30 Schalberg; 31 Madona dell'arma; 32 Fate; 33 Tasso; 34 Iena; 35 Cucigliana; 36 Gavardo; 37 Golino a Talamone; 38 Ponte di Veia; 39 Cassino; 40 Oida; 41 Taddeo; 42 Torre di Talao; 43 Tischoferhöhle; 44 Badelhöhle; 45 Gudenus-Höhle; 46 Teufelslucken; 47 Merkensteinerhöhle; 48 Windener Höhle; 49 Kartstein; 50 Herne i. W.; 51 Feldhofhöhle; *52* Göpfelsteinhöhle, Haldenstein, Sirgenstein-Höhle, Ursprung; 53 Buchberg; *54* Bockstein, Brillenhöhle, Irpfelhöhle, Vogelherd, Kleine Ofnet, Große Ofnet; 55 Osterode; *56* Velburger Schloßberg, Räuberhöhle, Schulerloch, Altendorf; 57 Gaillenreutherhöhle; 58 Hohler Fels; 59 Zwergloch; 60 Höhle bei Brumberg; *61* Dürrloch, Weinberghöhlen; 62 Hermannshöhle; *63* Ehringsdorf, Taubach; *64* Ilsenhöhle, Bad Köstritz, Lindenthaler Hyänenhöhle, Kalksteinbrüche; 65 Wschodnia (=Hellmich-cave); 66 Radochowska (=Reversdorfer cave); *67* Nad Kačákem, Sankt-Prokop-Höhle, Turská maštal, Zlatý kůň; 68 Český Krumlov, *69* Barová, cave no. 4, Eliščina, Kůlna, Nicová, Sklep, Vranův mlýn; *70* Pod hradem, Slouper, Žižka-cave (Žižkůvka, Žižkova díra, Na Končinách), Švédův stůl, V Hložku (Pod Vintokami), Výpustek; *71* Ćertova díra, Hranice, Předmostí, Šipka; 72 Dzeravá skála (Pálffy-cave); 73 Silická Brezová; *74* Betalov spodmol, Črnikal, Kanegra, Parska golobina, Postojnska jama, Romualdo, Sečovlje, Vela Spilja; *75* Krapina, Veternica, Vindija; *76* Brini, Pisana stina; 77 Srednji Lipovac; 78 Durkovina; 79 Risovača; 80 Makarovec; 81 Tokod-Nagyberek; *82* Csákvárer-Höhlung, Érd, Estérházy, Jankovich, Kiskevélyer, Szelim, Dorog, rock shelter no. 1 of Pilisszántó, rock shelter of Remetehegy, Süttő, Tarkő rock shelter, Tata; *83* Balla, Büdöspast, Diósgyörer cave, Hermans-cave (Herman-Ottó-cave, Istállóskö, Kálmán-Lambrecht, Lökvölgyer, Mexicovölgyer, Peskö, Subalyuk, Szeleta, Hórvölgy cave, Varbó; 84 Igric; 85 Magura; *86* Bordul-Mare, Spurcata; *87* Adam, Bordeiul de Piatra, Bursucilor, Izvor; 88 Devetaškata; *89* Morovica, Pešč, Vasil Lewski; 90 Petralona; 91 Sinjakowe; 92 Butešty; 93 Vychwatincy; *94* Nerubaj, Staroselje; *95* Adži Koba, Sjuren I; *96* Koš-Koba, Kiik-Koba, Ilskaja, Asych, Taglarskaja; 97 Ust-Katawska; 98 Tornewton cave; 99 Sandford Hill; 100 Pin Hole; *101* North sea findings; 102 Koziarna; 103 Raj; *104* Prima I, Lviv VII;

2 Methods

2.1 Sinal cavities

Nasal and frontal sinuses are present in every mammal. They comprise of cavities of different size and shape around the nasal and frontal skull bones. Lined with mucous membrane however they have no part in actual smelling. The function of these special traits is not fully researched and understood, but many theories exist. The most prominent of these are weight reduction and size extension of the skull, buffer zones against blows and thus increased protection for the brain, pressure and temperature buffers for sensitive organs in direct proximity to the nasal cavity (for example the eyes), enlargement or shape of inserting zones for facial muscles, warming of the inhaled air and noise creation. There is however no proof that one of these possibilities is the sole application for which the nasal and frontal sinuses developed.

2.2 Data acquisition

Computer tomography is a radiographic examination method which has been used for decades in medical investigation. The main difference compared to normal x-ray analysis lies in the data generated. A normal radiograph of an object is a two-dimensional image of a three-dimensional object, whereas a CT-scan produces many images virtually cutting the object in many layers. These so-called "slices" can then be combined to a virtual three-dimensional object for further investigation. In medicine usually the slices are used as is, to examine the medical condition of the patient. The 3D-reconstruction is mostly used in the anthropological field of application. The main advantage of computer tomography in inanimate research compared to other examination methods is its non-destructive nature which does not affect the analysed specimen in any way. In addition, the digital data produced my computer tomographs is ideal for sharing with other scientists due to the fact that digital files are easy to copy and they produce an exact reproduction of the investigation conducted.

Because of these advantages, this method was the perfect tool for mapping the nasal sinuses and cranial capacity of the hyaenid skulls. To measure the cranial capacity one could also fill the skull with mustard seed which is the usual method, but that could not be done with the frontal and nasal sinuses. For a long time, the only way to acquire data from these skull traits was by opening the skull along the midsagittal plain and thus severely damaging or even destroying the specimen. Especially for precious specimens

this was not an option (and all of the *Crocuta crocuta spelaea* skulls are in this group).

The digital double created by computer tomography is only limited in its quality by the resolution of the tomograph used. There is also no colour information included in the scans, but that is irrelevant for this study and therefore can be ignored.

2.2.1 Roentgen technology

The image generating method used in computer tomography is the roentgen technology discovered in 1895 by Wilhelm Conrad Röntgen in Würzburg[1]. X-rays are produced by accelerating electrons in a vacuum tube from a cathode towards an anode. Because of collision with the anode (usually a metal plate) the electrons are suddenly decelerated and knock out electrons from the inner shell of the metal atoms of the anode. Then electrons from higher energy levels in the atom fill up the vacancies, producing x-ray photons in the process. The x-rays are able to pass through compact matter and can be detected on a photographic plate. The more photons arrive at the photo-plate, the darker it gets. So in places, where the objects density stops more photons, the photo-plate remains brighter. Knowing this, it is possible to generate a two-dimensional image of the examined object including its interior shape! The image created is a grey scale image where the darker colours down to black represent less dense material (especially air) and the brighter colours up to white represent the more dense material. Here it is very important to know that the image has an angle non-conformity and therefore any measurements have to be corrected. Because of this problem, it was more often used to depict the interior of the scanned object for descriptive use only.

As x-rays are ionizing radiation it is possible to cause cellular mutations in living tissue. Because of this danger it is imperative to use radiation protection when working with x-rays. When the technology was discovered these dangers were unknown, and many people using x-rays in everyday life became ill and died of the radiation. The best protection is distance because x-ray intensity is reduced by the power of 2 by range. Lead plates and leaden aprons are also used as protection because they absorb x-rays very well. The most dangerous type of radiation are the soft x-rays which can cause grave cellular damage and are therefore mostly absorbed by aluminium shields inside the roentgen tube and have no part in the image creation.

After its discovery by Röntgen many fields of application where found for the new technology, and not only in scientific research, but also in everyday life. The first anthropological research was conducted on Neanderthal fragments from Krapina in 1902. In 1906 there was another review of Neanderthal fragments in the course of comparison of Neanderthal teeth with teeth from *Homo sapiens* (because there are differences in the dental pulp of these two species).

The possibility to look "inside" otherwise closed objects without destroying them was very inspiring. It was possible to analyse rare and precious unique specimens without

---

[1]Though Röntgen is known as the discoverer, x-rays had been produced much earlier. Some of the people who generated x-rays were Nikola Tesla in 1887 who conducted experiments with cathode ray indicator tubes, and Johann Hittdorf and William Crookes, who developed cathode ray indicators which where used by Röntgen himself.

damaging them and thus gain new knowledge about the subjects.

2.2.2 Computer tomography

Computer tomography itself is an enhanced application of the older x-ray technology and produces a three-dimensional image of the examined object through a multitude of directed and digitally analysed slices.

To generate the picture the computer uses a mathematical integral transform developed in 1917 by an Austrian mathematician by the name of Johann Radon. The inversion of this so-called "Radontransform" makes the calculation of the pictures out of the raw data possible.

The computer tomograph has a rotating array of roentgen tubes and detectors which produce mainly one-dimensional, orientated raw data. By using the radontransform all the raw one-dimensional scans of one complete 360°rotation can be reduced to a single two-dimensional image which resembles a radiograph in many ways. The definition (taken from Beyerer and León (2002), translated) of the radontransform is as follows:

The radontransform $r(u, \varphi) = \mathcal{R}\{b(\mathbf{x})\}$ of a signal $b(\mathbf{x}) = b(x_1, x_2)$ at the location $\mathbf{x} = (x_1, x_2)^T$ is defined as:

$$r(u, \varphi) = \mathcal{R}\{b(\mathbf{x})\} := \int\limits_{-\infty}^{\infty} \int\limits_{-\infty}^{\infty} b(\mathbf{x})\delta(\mathbf{x}^T\mathbf{e}_\varphi - u)\mathrm{d}\mathbf{x}$$

with

$$\varphi \in (0, 180), \qquad u \in \mathbb{R}, \qquad \mathbf{e}_\varphi = \begin{pmatrix} cos\varphi \\ sin\varphi \end{pmatrix}.$$

The δ-straight line

$$\delta(\mathbf{x}^T\mathbf{e}_\varphi - u)\text{"} = \text{"} \begin{cases} 0 & \text{for } \mathbf{x}^T\mathbf{e}_\varphi - u \neq 0 \\ \infty & \text{for } \mathbf{x}^T\mathbf{e}_\varphi - u = 0 \end{cases}$$

which works as transformation kernel makes sure that the signal $b(\mathbf{x})$ along the straight line with parameters u (source distance) and φ (straight line angle) are added together.

The radon back-transform is:

$$b(\mathbf{x}) = \mathcal{R}^{-1}\{r(u, \varphi)\} = \frac{1}{2\pi^2} \int\limits_{0}^{\pi} \int\limits_{-\infty}^{\infty} \frac{1}{(\mathbf{x}^T\mathbf{e}_\varphi - u)} \frac{\partial r(u, \varphi)}{\partial u} \mathrm{d}u\mathrm{d}\varphi$$

the back-transform delivers the signal $b(\mathbf{x})$ at given projection data $r(u, \varphi)$.

With these mathematical formulas it is possible for the computer to produce images out of raw x-ray data which would otherwise be only normal radiographs. It was not of import to fully understand the mathematical formulas given here, in order to work on the digital data-sets, but it should complete the information on the subject of computer tomography. For me myself only the finished scans and the methods of data acquisition were important.

The first prototypes of computer tomographs were developed by Sir Godfrey Newbold Hounsfield in 1970, and in 1971 he scanned the first human test-subject. In 1974 the SIRETOM — the first mass-produced computer tomograph — was constructed by Siemens. In 1979 the Nobel prize for medicine was presented to Hounsfield and the physicist Allan McLeod Cormack (whose work formed the basis for Hounsfield).

The first anthropological use of a computer tomograph was in 1980 when Jan Wind scanned a fragment of *Homo erectus* (Wind, 1980). Only four years later was the first palaeontological use by Glenn C. Conroy and Michael W. Vannier who scanned a sediment filled skull of *Stenopsochoerus* (Conroy and Vannier, 1984).

The first computer tomographs were large machines and much harder to use than now. Because of its size it was not possible to rotate the x-ray tube around the patient, but the patient had to rotate in the scan-area. That produced much more interference in the scans because of slight displacement of the patient. Today it is the other way around, and the patient is lying immobile on a table that glides slowly through the computer tomograph, and the roentgen tubes with detectors opposite to them rotate around the table and the patient (see also figure 2.1).

For this study the CT-images used were single slice scans, which means the table with the specimen was moved to a defined position and then the scan started. For each scan the roentgen tubes had to rotate a full 360°. After scanning a single slice, the table moved a defined distance (the slice thickness) and the next slice was scanned.

Modern computer tomographs used in medicine also have the option of a spiral-scan which works without stopping the table with the patient. The tomograph records the raw data as a spiral with an always slowly moving patient. The main advantages of this method are the shorter examination times and the lesser radiation exposure to the patient. A computer has to generate single slices out of this spiral-data. That results in slightly lesser resolution, but works much faster and by that has less interference by patient displacement. However, as the hyaena-skulls did not move that much any more, I could resort to the more precise single slice scan method.

The most advanced computer tomographs in use today can also scan multiple slices at once and are able to produce real time images of the scanned object which means 25 images per second! With such devices it is even possible to see the organs at work in real time (for example heart activity).

2.2.3 Equipment and procedure of data acquisition

For the data acquisition in this work different computer tomographs with different calibrations were used.

The main part was scanned at the University of Veterinary Medicine Vienna. That
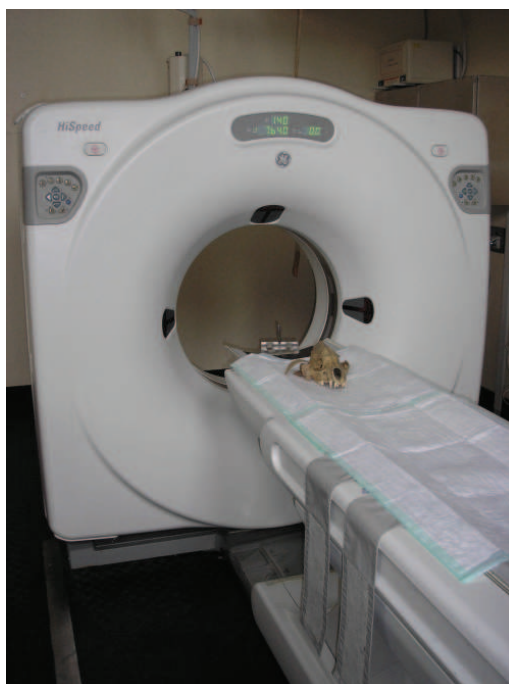
Figure 2.1: The spiral CT of the University of Veterinary Medicine Vienna

means all but one[2] *Crocuta crocuta crocuta* both *Hyaena hyaena* and three[3] of the *Crocuta crocuta spelaea* specimens have been digitized there. The tomograph there was a *General Electric CT Pace* spiral-CT. The scans where made with a 512×512 matrix and 1mm slice thickness, which was the best resolution possible on this tomograph. The raw data was computed by two different indexing methods, one focusing on soft tissue and the other focusing on bone. I used the bone index for my later work, because it had, as expected, much sharper borders from air to actual tissue. To save time and conserve the durability of the machine, each specimen was scanned without its zygomatic arches because they were not essential for later measuring. Each specimen was scanned in full length and height in a lateral view. The width of the scan depended on each individual specimen, but consisted usually from the left to the right processus zygomaticus. Exact information for each specimen is given in chapter 4.

The skull with inventory number 1373 had been scanned by the Department of Anthropology of the University of Vienna some years ago at the Universitätsklinik Innsbruck. Along with it, the fossil specimen with inventory number III from Eggenburg had also been scanned there. Both scans comprise of the complete skull including the zygomatic arches (although these are also absent in the Eggenburg-specimen because they were not fossilised) and were made in transverse view. The tomograph used there was a *Simens Somatom Plus 40*. The settings for specimen 1373 were set to a 512×512 matrix with 0,3mm slice thickness, and for specimen III to a 512×512 matrix with a thickness of 1mm.

---

[2]Specimen No 1373
[3]Specimens No 7801, 21459 and IPB M 432

The specimen number 6617 from the Löwentormuseum in Stuttgart was scanned at the Katharinenhospital in Stuttgart because it was on display at the museum and could not be removed from its place for long. The computer tomograph used there was a *General Electric Lightspeed* 4-row[4] multislicer. The specimen was scanned with a 512×373 pixel matrix and a slice thickness of 1,25mm. It was also scanned completely with both zygomatic arches, and in coronal view.

For this work the relevant part of the skull was situated around the cranial region (consisting of frontal bone, parietal bone and parts of the temporal bone) and the crista dorsalis starting at the opisthocranium and arcing along the median sagittal plain down to the nasal bone. See also the schematic in figure 2.2.
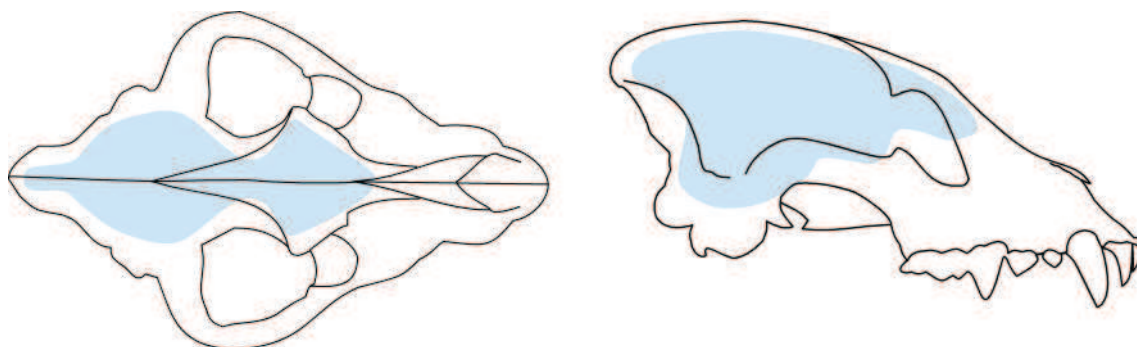

Figure 2.2: Sketch of generalised hyaenid skull in dorsal view (left) and lateral view (right); regions marked in light blue colour are the relevant parts for this study (sinal cavities and endocranial cavity).

2.2.4 Software used

To get the relevant data from the scans, it is now essential to edit each single slice by hand. To do this I used the software *Analyze 4.0* from AnalyzeDirect, Inc., Mayo Foundation which was provided along with a computer and the corresponding software licence by the Department of Anthropology in Vienna.

The work is actually quite simple but takes much time to complete and one has to get accustomed to the quirks of the software. The data-set is, as mentioned before, composed of many grey scale images where the scale reaches from complete black for the least dense material (in my case air) to white for the most dense material (in my case bone and dental enamel). The count from black to white is always different depending on the computer tomograph and the settings for the scan and normally reaches from about -2000 (for maximum black) to +3000 (for maximum white) in a not further known scaling environment. So first of all it was necessary to bring all scans to the same condition. Every scan was reduced to a colour range from 0 (for maximum black) to 4095 (for maximum white) for further handling. When that was done, the scans had to be prepared in a special way. The maximum white value of 4095 was reduced to 4094

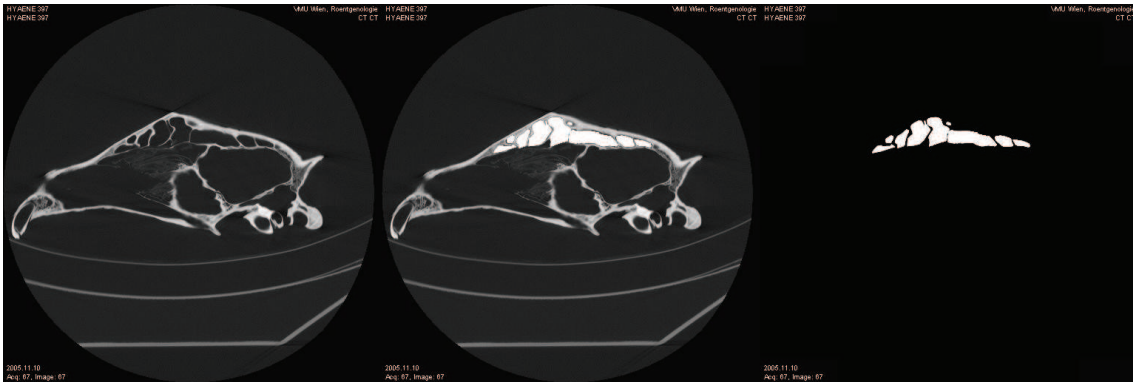[4]Four slices could be scanned simultaneously

Figure 2.3: Sample slice of a CT-scan demonstrating the necessary work. **Left** - slice no 67 from the ct data-set of specimen 397, **middle** - the white-filled sinal cavities, **right** - everything else is reduced leaving only the filled cavities for measurement.

to leave the value of 4095 unused in the data-set. That results in the loss of a little information concerning density of dental enamel to bone, but this is not important for the further analysis. On the other hand it is necessary, because to measure volume the software can only use a density value or range of values actually existing in the data-set. After these preparations it is possible to digitally fill the endocranium or the nasal sinuses with this free density value to measure the volume of the hollow spaces.

To do this, every single slice has to be edited separately, to fill the required cavities with this white value. To choose the right threshold between bone and air the half maximum height (HMH) method was used. This method has been approved in virtual anthropology to produce the most reliable data, compared with established volume measuring methods (Weber et al., 1998). To decide the right threshold a couple of line profiles are laid through a slice of the data-set and the mean grey value is recorded for every line profile. The average of these values is the threshold that should be used for this data-set to produce the most reliable data.

To get different "virtual endocasts" of the sinuses and the endocranium it is necessary to work on two different files of the same data-set. It is not possible to work on one file and later differentiate the endocasts. For example after finishing the endocranial work the work on the sinuses has to be done on a new copy of the original unchanged (but prepared) data-set.

To fill the cavities with the 4095 value, the software has some helpful automatic mechanisms but it is nearly always important to rework it by hand. This is very important at points where channels or other openings interchange with the cavities, because those gaps are not automatically recognized by the software. Therefore it is essential to study the skull anatomy before starting to work, to differentiate the cavities of the nasal sinuses from such features. It requires a little experience and good spatial sense to locate such three-dimensional bodies in the two-dimensional slices of the computer tomograph. Additionally with fossil data it is often not possible to use the automatic tools, because the cavities are often filled with sediment and therefore

the contrast to the bone is not large enough for the computer to identify.

After filling all cavities of one slice with the maximum white value, work proceeds to the next slice. After finishing all the slices of one data-set, the software can measure the volume of all areas with the value of 4095 and produces the cranial or sinal volume data for this specimen. The volume data can be measured because the height and breadth of every voxel is known, and the depth is given by the distance of the slices. Thus the software only sums up all the voxels with the defined 4095 white value to generate the volume data of the complete endocast.

After obtaining the volume data from all the edited specimens the next step was to acquire distance data from the surface of the specimens, to mutually correlate the volume data. This was achieved using the software *Amira 3.1* from Mercury Computer Systems. Here it was possible to remove unwanted artefacts from the scans (for example the examination table on which the specimens were placed in the computer tomograph) to produce clean, freefloating 3D-reconstructions of the skulls for further investigation. Prior to that some measuring points on the skulls were chosen. The requirement for these points was, that they had to be easy and exact to locate and their location had to be reproducible. The chosen points were all located on the median sagittal plain. The definition of all the points is given at the end of chapter 4 and in the glossary.

After deciding which points to use, landmarks where set in *Amira* at their locations on every specimen to make later reviewing easier. The distances between the points have then been measured from these landmarks. To verify the credibility of the digital distance measurements, some chosen distances have been verified on the real skulls with conventional methods. Furthermore the mean of absolute difference has been calculated for both methods. More information about this can be found in the respective detailed specimen descriptions in chapter 4.

2.3 Measured specimens

Below is a list of the specimens used in this study, including all information that was available on each subject beforehand. Shown in figure 2.4 are the locations (if known) of each specimen's discovery. Exact morphological descriptions of all of the specimens are given in chapter 4.

2.3.1 Museum of Natural History Vienna

Inventory No 397 *Crocuta crocuta*, adult, sex not verified; eastern South Africa (Orange Free State - Zambia); 1883-1887; Dr. Emil Holub leg. et don. (AV 1894/II/2)

Inventory No 1150 *Crocuta crocuta*, adult, sex not verified; Masai-Highland, province Arusha, Tanzania; 1899/1900; Prof. C. G. Schillings leg. et don. (AV 1900/II/15a)

Inventory No 1244 *Crocuta crocuta*, adult, sex not verified; eastern South Afrika (Orange Free State - Zambia); (1883-1887); Dr. Emil Holub; bought from his estate in 1903 (AV 1903/II/22); DNA sample of right I_1, Dr. Doris Nagel, 22.05.2002

Figure 2.4: Map representing finds of measured specimens. Spades indicate recent hyaenids (*Crocuta crocuta crocuta* and *Hyaena hyaena*), circles indicate fossil specimens (*Crocuta crocuta spelaea*).

Inventory No 1744/B *Crocuta crocuta*, adult, sex not verified; at Setit river near Sudanese border (= about Homera), province Begemdir or Semyen, Ethiopia, 14°15' north / 36°40' east; 1907; Němec / Benschau leg. et vend. (AV 1907/XIII/(1))

Inventory No 1755 *Crocuta crocuta*, age unknown, female; Somaliland (= British Somalia, now North Somalia, presumably at the Berbera-Hargeisa range); 1898; Němec leg.; bought 1907 (AV 1907/XIII/(1)); DNA sample of left I_1, Dr. Doris Nagel, 22.05.2002

Inventory No 1756 *Hyaena hyaena* (*Hyaena hyaena dubbah* F. A. A. Meyer 1793), age unknown, sex not verified; Somaliland (= British Somalia, now North Somalia, presumably at the Berbera-Hargeisa range); 1898; Němec leg.; bought 1907 (AV 1907/XIII/XIII); DNA sample of left M_1, proximal root, Dr. Doris Nagel, 22.05.2002

Inventory No 2531 *Hyaena hyaena*, age unknown, sex not verified; 1863; Tiergarten Schönbrunn don. (in Av 1863/XII and XIV not listed in the "Schönbrunn-Zugängen", but recorded in ZK Skel.); DNA sample of left P^2, distal root fragment, Dr. Doris Nagel, 22.05.2002

Inventory No 3919 *Crocuta crocuta*, adult, sex not verified; Stony Athi, 1°36' south / 37°0' east, Kenya; 2nd of October 1908; Dr. Horaz Sonnenthal leg. (came into possession of the Museum of Natural History Vienna presumably in 1920 along with his estate, though listed in AV 1920/XII are only antelopes and native ungulates); DNA sample of right I^1, Dr. Doris Nagel, 22.05.2002

Inventory No 5584 *Crocuta crocuta*, adult, male (?); Ngalhni/Sigare (n. lok.), province North, Cameroon; 9th of Mai 1933; E. A. Zwilling leg et don.; DNA sample of left I_3, Dr. Doris Nagel, 22.05.2002

Inventory No 6061 *Crocuta crocuta*, adult, sex not verified; upper reaches of river Dinder between Abu Hashim and Hegeirat, Blue Nile province, Sudan; 1925; Prof. Dr. H. A. Bernatzik leg. et don.; DNA sample of right M_1, distal root, Dr. Doris Nagel, 22.05.2002

Inventory No 6062 *Crocuta crocuta*, adult, sex not verified; upper reaches of river Dinder between Abu Hashim and Hegeirat, Blue Nile province, Sudan; 1925; Prof. Dr. H. A. Bernatzik leg. et don.; DNA sample of right I_1, Dr. Doris Nagel, 22.05.2002

Inventory No 6063 *Crocuta crocuta*, adult, sex not verified; upper reaches of river Dinder between Abu Hashim and Hegeirat, Blue Nile province, Sudan; 1925; Prof. Dr. H. A. Bernatzik leg. et don.; DNA sample of right I^3, Dr. Doris Nagel, 22.05.2002

Inventory No 6064 *Crocuta crocuta*, adult, sex not verified; upper reaches of river Dinder between Abu Hashim and Hegeirat, Blue Nile province, Sudan; 1925; Prof. Dr. H. A. Bernatzik leg. et don.

Inventory No 7393 *Crocuta crocuta*, adult, male; Beni, 0°26' north / 29°35' east, province Kivu, Kongo/Zaire; July, 1910; Prof. Rudolf Grauer leg. Ph. v. Oberländer don.

Inventory No 7397 *Crocuta crocuta*, adult, sex not verified; southern shore of lake Chad, province North, Cameroon; (1928-38); E. A. Zwilling leg. et don.

Inventory No 21495 *Crocuta crocuta*, adult, sex not verified; Wadelai (now Mutir), 2°34' north / 31°26' east, Uganda (labeled "upper Egypt"); (1882); Dr. Emin Bey leg. et don.; 1913 taken over from the geological-palaeontological department; right side of cranium sawn open; DNA sample of left P^2, proximal part, Dr. Doris Nagel, 22.05.2002

2.3.2 Department of Paleontology, University of Vienna

Inventory No 1373 *Crocuta crocuta*, adult, female; no place of origin given;

2.3.3 Krahuletz-Museum, Eggenburg

Inventory No III *Crocuta crocuta spelaea*, adult, sex not verified; Teufelslucken near Roggendorf; reviewed in Ehrenberg et al. (1938)

2.3.4 Löwentormuseum, Stuttgart

Inventory No 6617 *Crocuta crocuta spelaea*, age unknown, sex not verified; Ketsch, Krenzwiese; Schausammlung Quartär, carnivores – WV 3.6, 1985

Inventory No 7801 *Hyaena spelaea* Cuvier (= *Crocuta crocuta spelaea*), age unknown, sex not verified; Pleistocene cave sediment, Irpfelhöhle near Giengen an der Brenz (7327/03); 1892; Hermann Emil Sihler et. al.; reviewed in Fraas (1893)

Inventory No 19062 *Crocuta crocuta spelaea*, age unknown, sex not verified; Erkenbrechtsweiler; 1941; reviewed in Schwenkel (1950)

2.3.5 Goldfuß-Museum, Bonn

Inventory No IPB M 432 *Crocuta crocuta spelaea*, adult, sex not verified; Zoolithenhöhle near Burggaillenreuth, Franconia

3 Taxonomy

Although hyaenids may look much like dogs especially because of their facial features, they are systematically closer to cats. Their ancestors derived from the viverrids and their dental formula still shows their relationship to modern cats. This is the basic systematic position of all hyaenids:

Order *Carnivora*
    Family *Hyaenidae*
        Subfamily *Hyaeninae*
            Genus *Crocuta*
            Genus *Hyaena*
            Genus *Parahyaena*
        Subfamily *Protelinae*
            Genus *Proteles*

Crocuta and *Hyaena* have been used in this study and are discussed in detail below.

Parahyaena brunnea Thunberg (1820), the brown hyena, is the third species of the family but is even smaller than *Hyaena hyaena* and lives only in southern Africa. Its diet is based mostly upon carrion, plants and fruits.

Proteles cristatus Sparrmann (1783), the aardwolf, has developed a special ecological adaptation in its diet. It feeds singularly on termites. In contrast to other termite- and ant-eating animals, it lacks the ability to penetrate the termite mounds and thus is limited to feeding on the termites that appear on the surface. The aardwolf is the smallest of the extant hyaenids.

Because of their importance in this study, the following discussion of *crocuta* and *hyaena* is more detailed.

3.1 *Crocuta crocuta crocuta*

The synonyms of *Crocuta crocuta* Erxleben (1777) are listed completely in Werdelin and Solounias (1991). Its recent habitat is limited to Africa; that lies in extreme contrast to its fossil record, which consists of specimens found all over Europe and Asia. These fossils are mostly subspecies and are genetically nearly identical to *Crocuta crocuta crocuta* as presented in Hofreiter et al. (2004) and Rohland et al. (2005).

The spotted hyena *Crocuta crocuta crocuta* is the largest existing hyena today and lives in large family-like clans of up to one hundred individuals led by a dominant female. In contrast to the general believe that hyenas are only scavengers, the spotted hyena is one of Africa's largest predators and hunts a great percentage of its food itself

(Kruuk, 1972). Clans of hyenas prowling near the feeding grounds of lions have often been interpreted as waiting for their chance to take the lion's prey, but the opposite is more often the case! The larger lions wait for the hyenas to do the killing, and scare them away afterwards to feed. The lifestyle of spotted hyenas is extensively discussed in Kruuk (1972). Hyenas communicate through a series of growls and yelps, which sometimes sound like human laughter, this gave them the name "laughing hyena". There is no known sexual dimorphism in any hyenas (including the following species) which is discussed in Werdelin and Solounias (1991).

The dental formula of *Crocuta crocuta crocuta* is $\frac{3140}{3141}$.

3.2 *Crocuta crocuta spelaea*

The cave hyena *Crocuta crocuta spelaea* is a fossil hyena often found in European caves. The recent opinion is that the cave hyena is actually a subspecies of *Crocuta crocuta* called *Crocuta crocuta spelaea*. The species status proposed by Ehrenberg et al. (1938) was induced because of large differences in fore and hind extremities compared to common *Crocuta crocuta* but Kurtén (1956) writes "[...] there is evidence that this European population was continuous with southern, typical representatives of the nominate subspecies". However there was the discussion by some authors (Markova et al., 1995; Baryshnikov, 1999) about elevating the cave hyena to its own species status, but the genetic analysis made by Hofreiter et al. (2004) indicates no difference in the DNA of *Crocuta crocuta spelaea* and *Crocuta crocuta crocuta*.

The main distinction between the recent *Crocuta crocuta crocuta* and the fossil *Crocuta crocuta spelaea* is grounded on different lengths of the hind and fore limb bones. In *Crocuta crocuta spelaea* a length reduction in the distal extremities (metapodes) with synchronous length increase of the proximal limb parts (humerus and femur) indicates the adaptation to a different habitat than the recent *Crocuta crocuta crocuta*. The middle limb parts (radius & ulna and tibia & fibula) show no change in size.

The real lifestyle of cave hyenas is not known and can only be speculated about. The changes in limb proportions indicate a different adaptation to the typically running *Crocuta crocuta crocuta* of modern Africa. Also the caves as living space is widely accepted. It is not known if there was also no sexual dimorphism in fossil hyenas as is the case in recent ones, and there is also no indication if cave hyenas lived in large clans or on a more solitary basis, though in their Pleistocene habitat large clans are not very likely.

The dental formula of *Crocuta crocuta spelaea* is also $\frac{3140}{3141}$, like all specimens of *Crocuta crocuta*.

3.3 *Hyaena hyaena*

The synonyms of the striped hyena *Hyaena hyaena* Linnaeus (1758) are given in detail in Werdelin and Solounias (1991). The habitat of the striped hyena has expanded from Africa probably in very recent times because of the missing fossil record (Werdelin and

Solounias, 1991). The small genetic variation in worldwide examples also indicates a very recent expansion possibly down to neolithic times, as shown in Rohland et al. (2005). Today *Hyaena hyaena* can be found in addition to northern Africa, on the Arabian Peninsula, in Asia Minor and in India.

The striped hyena is much smaller than the spotted hyena and has only about half its body weight. Its lifestyle is quite different to its larger cousins. Because of its smaller body size it does not hunt large prey but lives mostly on carrion and small animals. It is also unable to produce sounds similar to the laughter of its larger relatives in Africa. Striped hyenas communicate through a series of different growls.

The dental formula of *Hyaena hyaena* is $\frac{3141}{3141}$. Compared to *Crocuta crocuta* in *Hyaena hyaena* the M^1 still remains.

4 Results

4.1 Description of Specimens

This chapter deals with detailed descriptions of all the specimens used in the study, and the computer tomographic settings they were scanned and edited with. Fossil specimens also include a short description about their place of discovery. There are also photographs of each specimen in dorsal and lateral view, along with digital images of the virtual endocasts of the sinal cavities. These endocasts are displayed without any angle non-conformity (because the digital focal distance is infinite, unlike the limits of real cameras and lenses) in contrast to the real photographs. Therefore they do not overlap exactly with the photographs, and may seem out of shape compared to the real skulls.

4.1.1 Specimen No. 397

The specimen is from the collection of the Museum of Natural History in Vienna. It is mostly complete, only missing both P^2. The skull is fairly large with an Inion-Prosthion distance of 287,18mm. The parietal bone has a well developed beak at the position of the Inion and spans across the median sagittal plain in a smooth arc. It joins the frontal bone at the Bregma and there the forehead descends in a small ravine to the Nasion along an average angle. The os nasale starts with this same angle at its dorsal end but arcs up changing its angle to become nearly parallel to the secondary palatum at its ventral end. The praemaxillar bone is then descending in a very steep angle to the Incisors.

The virtual endocast of the nasal sinus is well shaped and asymmetric. Its left hemisphere does not reach as far into the nasal region as its right hemisphere. Also the part of the endocast filling the left processus zygomaticus is smaller in development compared to the right processus zygomaticus.

The CT-scan was made at the University of Veterinary Medicine and consists of 105 slices at 512×512 pixels each. Each voxel has a real size of 0.625×0.625×1mm. The scan was made in sagittal view, the average HMH was 805.

4.1.2 Specimen No. 1150

The specimen is from the collection of the Museum of Natural History in Vienna. The skull has major damage around the foramen magnum and thus has lost the Basion and

the Opisthion, but it is not that grave as to interfere with measuring the endocranial volume. Its teeth are intact except the partially broken right canine. It is quite small with just 252.16mm from Inion to Prosthion. It has no beak developed at the position of the Inion where the sagittal crest is very thin and cantilevered, but it can be clearly defined at the meeting point of the superior nuchal lines. Starting at the occipital protuberance, the parietal bone arcs along the median sagittal plain very smoothly. There is no change in the angle of the arc where the parietal bone joins the frontal bone and even at the nasal bone there is just a very slight upward slope. Due to its overall shortness, the skull seems much broader in transverse view.

The virtual endocast of the sinal cavities is very broad developed overlying the cranial region. The filling of the right processus zygomaticus is gone due to an injury to the processus. But also the filling of the left processus zygomaticus is very thin. The overall shape of the endocast in lateral view is very smooth.

The scan was made at the University of Veterinary Medicine and consists of 83 slices at 512×512 pixels each. Each voxel has a real size of 0.586×0.586×1mm. The scan was made in sagittal view, the average HMH was 950.

4.1.3 Specimen No. 1244

The skull is from the collection of the Museum of Natural History in Vienna. It is missing its right canine which probably has been lost in life because the alveolus has been closed. The distance from Inion to Prosthion represents an average skull length with 267,73mm. The Inion is defined by a slight, but unmistakable beak and from there the skull extends just barely to the occipital protuberance. There it arcs along the sagittal crest in an angle that smooths very soon along the parietal bone and joins the frontal bone without change. The nasal bone curves up very slightly but the praemaxillar bone picks up the angle again and directs it down to the Prosthion. Viewed from the transverse the skull looks very narrow just behind the processi zygomatici and its Bregma is located very near the Nasion compared to other specimens (see also the distances shown in Table 4.2).

The virtual endocast of the nasal and frontal sinuses looks very rounded compared to other endocasts. Its asymmetric, with a slightly larger developed left hemisphere. Nevertheless both processi zygomatici have no prominent fillings. In lateral view the distal end of the endocast looks very rounded, and in dorsal view its thinning out cone-shaped.

The scan was made at the University of Veterinary Medicine and consists of 97 slices at 512×512 pixels each. Each voxel has a real size of 0.586×0.586×1mm. The scan was made in sagittal view, the average HMH was 867.

4.1.4 Specimen No. 1373

This specimen is from the Institute of Paleontology, University of Vienna. The skull itself is mostly complete, only missing a small part of its left canine and its left bulla auditoria. It is the smallest specimen of *Crocuta crocuta crocuta* with a Inion-Prosthion
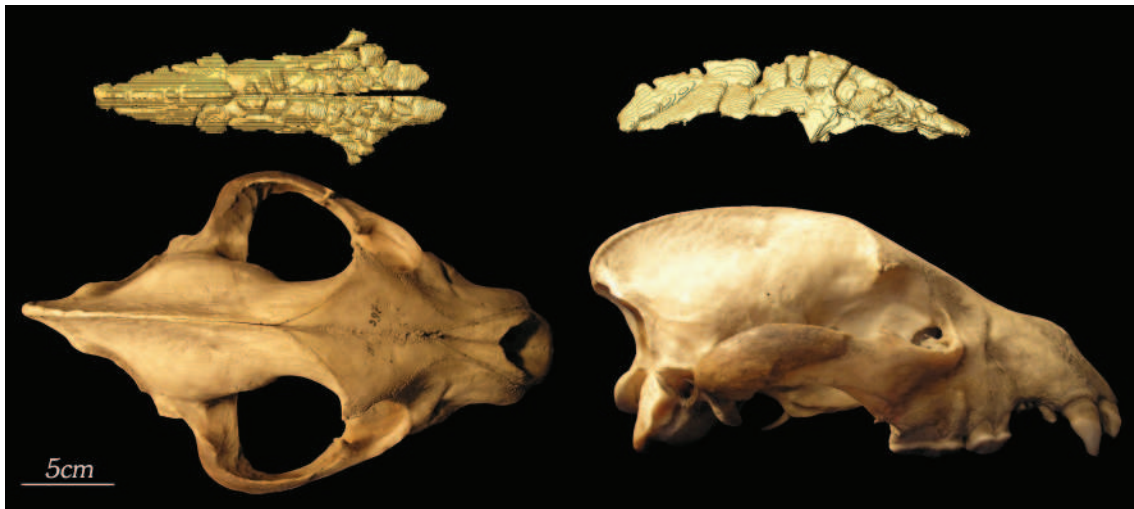
Figure 4.1: Specimen No. 397, *Crocuta crocuta crocuta* from the Museum of Natural History Vienna. Virtual endocast of sinal cavities and photo of actual skull in dorsal (left) and lateral (right) view.

Figure 4.2: Specimen No. 1150, *Crocuta crocuta crocuta* from the Museum of Natural History Vienna. Virtual endocast of sinal cavities and photo of actual skull in dorsal (left) and lateral (right) view.

distance of just 237,14mm. It has a mediocre sagittal crest at its occipital end, and the typical arc along the median sagittal plain has two disturbances along its way. One located a little above the Nasion where the skull builds a small protrusion and the other at the end of the nasal bone at the usual point, where the nose changes the angle of the arc a little upwards. The praemaxillar bone arcs down to the Prosthion again a little steeper. In transverse view the Bregma is positioned very far from the Nasion and closer to the Inion which smooths the angle of the curve the frontal bone develops along the pars temporalis.

The virtual endocast of the sinal cavities is overlying the whole cranial section of the skull, thinning out in its distal region cone-shaped. Its asymmetric with a better developed filling of the right processus zygomaticus. In lateral view the distal end of the endocast looks more pointed than in other specimens.

The scan was made at the Universitätsklinik Innsbruck in the year 2002 by the Department of Anthropology of the University of Vienna, but the acquired data has not been used in any publication since, except a poster at the 12th RCMNS conference in Vienna, Autumn 2005. The scan is complete, including both zygomatic arches. It consists of 479 slices at 512×512 pixels each. Each voxel has a real size of 0.488×0.488×0.3mm. The scan was made in transverse view, the average HMH was 530.

4.1.5 Specimen No. 1744/B

The specimen is from the Museum of Natural History in Vienna. It is well preserved, and is missing only a part of its left and right P^1 and its complete left P^2. The position of the Inion is not very well defined. The sagittal crest arcs along the parietal bone and the frontal bone joins at the same angle. There is a sharp bend at the position of the nasal bone where the angle changes upward to the position of the nose. Then it angles down again along the praemaxillar bone to the Prosthion. From top view the skull is very slender and narrow behind the position of the processi zygomatici.

The virtual endocast of this specimen is especially large developed. Its distal end is broad in lateral view, and surrounds a greater part of the cranial cavity than in other specimens. The endocast is very compact, and both processi zygomatici are filled very well. Although the left hemisphere does not reach as far into the nasal section as the right hemisphere.

The scan was made at the University of Veterinary Medicine and consists of 103 slices at 512×512 pixels each. Each voxel has a real size of 0.684×0.684×1mm. The scan was made in sagittal view, the average HMH was 781.

4.1.6 Specimen No. 1755

The specimen is from the collection of the Museum of Natural History in Vienna. It is in fairly good shape, only missing the left and right I^1 and with a small hole in the left bulla auditoria. The skull-length from Inion to Prosthion is average with 256,69mm. The sagittal crest is small and undeveloped. It arcs up from the Inion, along the median sagittal plain, not becoming taller in any position. A little dorsal of the Bregma, the
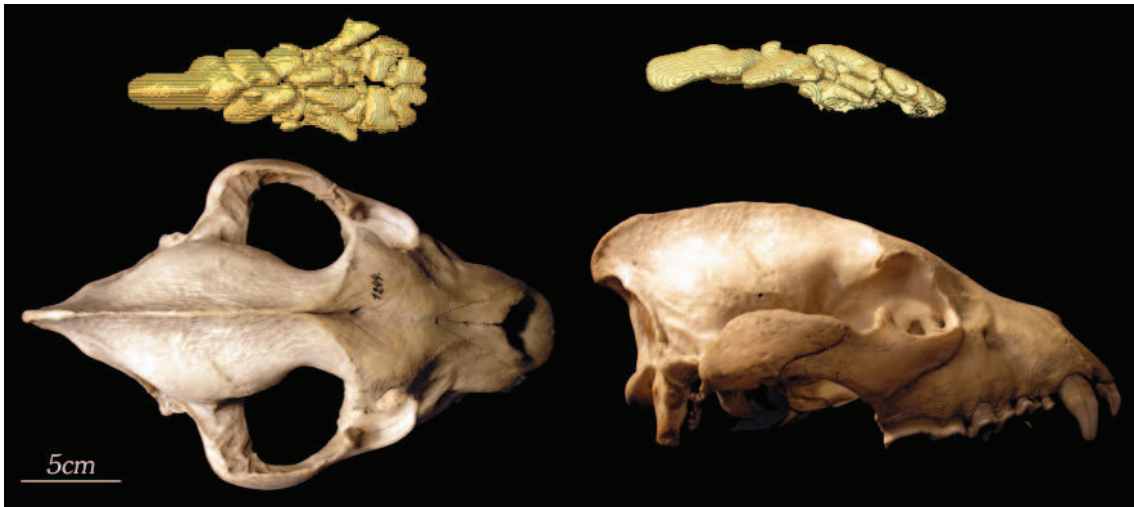
Figure 4.3: Specimen No. 1244, *Crocuta crocuta crocuta* from the Museum of Natural History Vienna. Virtual endocast of sinal cavities and photo of actual skull in dorsal (left) and lateral (right) view.
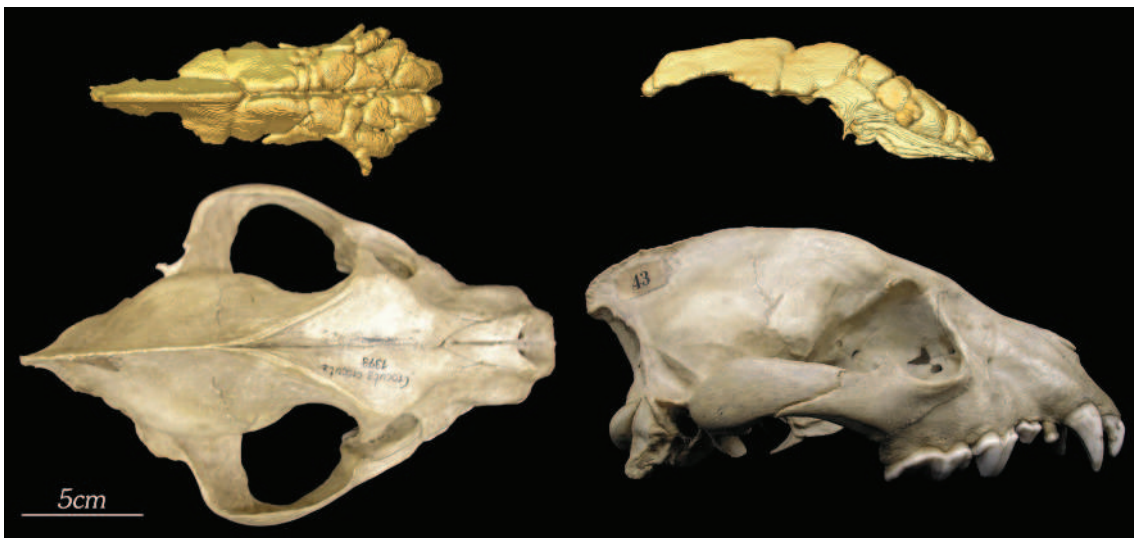

Figure 4.4: Specimen No. 1373, *Crocuta crocuta crocuta* from the Institute of Paleontology, University of Vienna. Virtual endocast of sinal cavities and photo of actual skull in dorsal (left) and lateral (right) view.

angle of the median sagittal plain goes down towards the Prosthion. It never really changes its angle, only a little bit at the nasal bone.

The hemispheres and parts of the virtual endocast of the sinal cavities are more separated by bony structures than in other specimens. The endocast also overlaps the cranial region not completely at the distal end.

The scan was made at the University of Veterinary Medicine and consists of 79 slices at 512×512 pixels each. Each voxel has a real size of 0.586×0.586×1mm. The scan was made in sagittal view, the average HMH was 1050.

4.1.7 Specimen No. 1756

The skull is from a *Hyaena hyaena* from the Museum of National History in Vienna. It is missing its right I[1] and, as a very special trait, has some healed up injuries on its left and right frontal bones. In the right frontal bone around the position of the Bregma is a hole of about 1cm in diameter and a second injury is located on the median sagittal plain, some 3cm oral of the Bregma. The larger part of the injury is located on the right frontal bone, but a little is also on the left frontal bone. It has not been verfied if this injury came from an attack against the hyena. It is however unquestionable that the injury healed up later, and was not responsible for the death of the animal. Compared to the specimens of *Crocuta crocuta crocuta* discussed until now, this skull is lower with a well developed sagittal crest. The skull is, as expected, very small with a Inion-Prosthion distance of 223,8mm. It has wide zygomatic arches which make the skull seem broader than *Crocuta crocuta crocuta*.

The virtual endocast of this specimen is cone-shaped on the distal side in dorsal view. In lateral view the whole endocast looks crescent-shaped with a small upthrust in the most distal region. Both fillings of the left and right processus zygomaticus are very large developed.

The CT-scan was made at the University of Veterinary Medicine and consists of 85 slices at 512×512 pixels each. Each voxel has a real size of 0.586×0.586×1mm. The scan was made in sagittal view, the average HMH was 900.

4.1.8 Specimen No. 2531

The second specimen of *Hyaena hyaena* used in this study is also from the Museum of Natural History Vienna. It was scanned with its lower jaw because the complete skull could not be disassembled. It is missing its left I[1-2] and P[2-3]. It also is missing both its M[1]. All other teeth look very used, and indicate an old individual. The distance from Inion to Prosthion is 233,03mm. The development of the sagittal crest is very similar to specimen No. 1756. From its highest developed dorsal part to the Bregma and a little further, it is nearly straight. Then it arcs down a little to the Nasion, where on the nasal bone the median sagittal plain angles up again. At the oral end of the nasal bone it arcs down again towards the Prosthion.

The virtual endocast overlaps the cranial region in the distal part very well. Around the processi zygomatici the endocast is very bulky. The crista dorsalis is large and thin
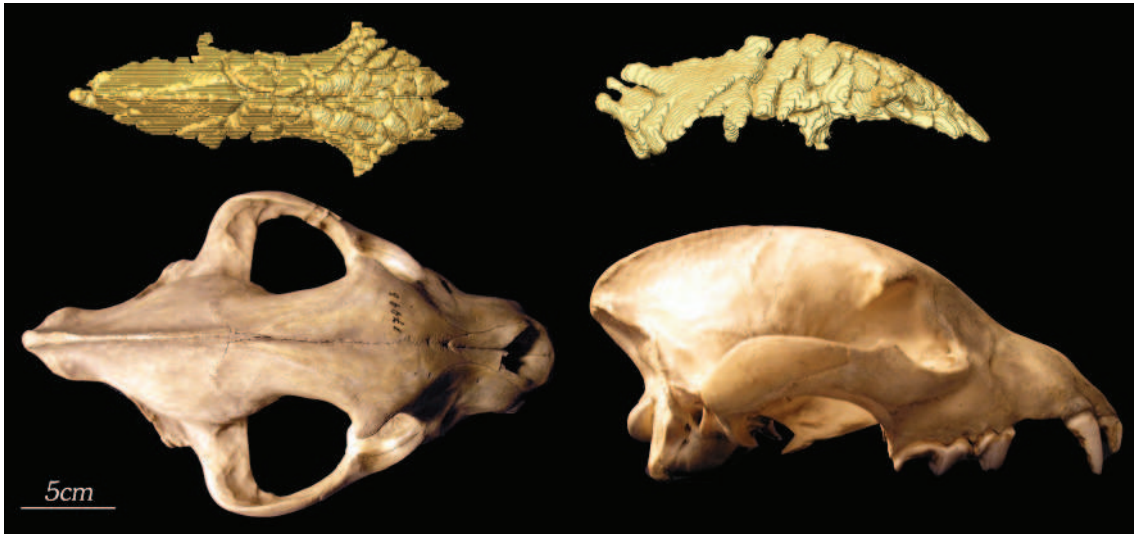
Figure 4.5: Specimen No. 1744/B, *Crocuta crocuta crocuta* from the Museum of Natural History Vienna. Virtual endocast of sinal cavities and photo of actual skull in dorsal (left) and lateral (right) view.

Figure 4.6: Specimen No. 1755, *Crocuta crocuta crocuta* from the Museum of Natural History Vienna. Virtual endocast of sinal cavities and photo of actual skull in dorsal (left) and lateral (right) view.

and the sinal cavities have only a very small part of it.

The scan was made at the University of Veterinary Medicine and consists of 74 slices at 512×512 pixels each. Each voxel has a real size of 0.586×0.586×1mm. The scan was made in sagittal view, the average HMH was 910.

4.1.9 Specimen No. 3919

Specimen No. 3919 is from the Museum of National History in Vienna. It is small, with a distance from Inion to Prosthion of only 247,70mm. It is missing its left I^2. Its right I^1 is longer than the other incisors, however the right I^3 is smaller than its left counterpart. All the other teeth are in good shape. The skull is slightly asymmetric between the Opisthion and the Inion favouring the right skull-side. The sagittal crest is symmetric again, but a little less developed than in other specimens. From the Bremga towards the Prosthion the median sagittal plain arcs down nearly straight only with a slight disturbance at the position of the nasal bone.

The virtual endocast is crescent shaped in lateral view, its distal part not pointed but broad developed. In dorsal view both hemispheres are nearly symmetric in size, but asymmetric in development of the structures.

The scan was made at the University of Veterinary Medicine and consists of 94 slices at 512×512 pixels each. Each voxel has a real size of 0.586×0.586×1mm. The scan was made in sagittal view, the average HMH was 770.

4.1.10 Specimen No. 5584

The specimen is from the collection of the Museum of Natural History Vienna. It is in perfect condition, neither missing a single tooth, nor suffering from other damage. The position of the Inion is perfectly visible because of a well developed beak, and the complete skull-length from Inion to Prosthion makes it, at 291.17mm, the largest specimen in this study. Viewed from lateral, it seams that a single arc spans along the median sagittal plain from Inion to Prosthion nearly undisturbed by the nasal bone, which extrudes a little out of the usual arc.

The virtual endocast of this specimen seems very large and in dorsal view cone-shaped towards its distal end. It looks very compact overall. Both processi zygomatici are well developed and completely filled.

The scan was made at the University of Veterinary Medicine and consists of 93 slices at 512×512 pixels each. Each voxel has a real size of 0.586×0.586×1mm. The scan was made in sagittal view, the average HMH was 880.

4.1.11 Specimen No. 6061

This skull is from the collection of the Museum of Natural History in Vienna. Its Inion-Prosthion distance is 272.80mm. The Inion can be positioned by a small but unmistakable beak at the dorsal end of the sagittal crest. The skull is missing its left I^{1-3} and its right I^{1-2} as well. It is also missing its right P^{1-2}. Otherwise the specimen
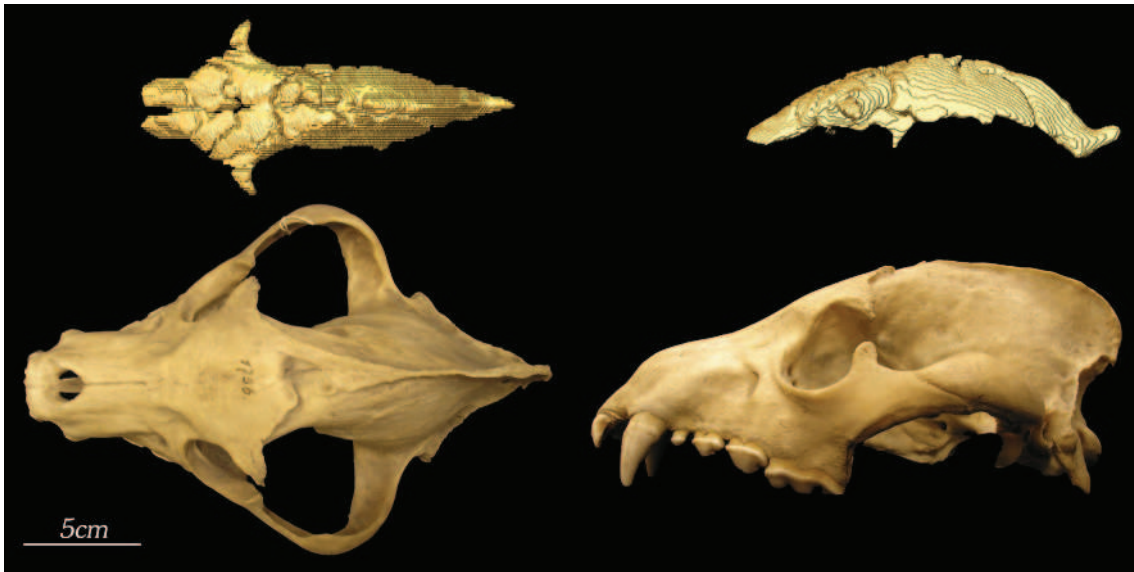
Figure 4.7: Specimen No. 1756, *Hyaena hyaena* from the Museum of Natural History Vienna. Virtual endocast of sinal cavities and photo of actual skull in dorsal (left) and lateral (right) view.

Figure 4.8: Specimen No. 2531, *Hyaena hyaena* from the Museum of Natural History Vienna. Virtual endocast of sinal cavities and photo of actual skull in dorsal (left) and lateral (right) view.

Figure 4.9: Specimen No. 3919, *Crocuta crocuta crocuta* from the Museum of Natural History Vienna. Virtual endocast of sinal cavities and photo of actual skull in dorsal (left) and lateral (right) view.

Figure 4.10: Specimen No. 5584, *Crocuta crocuta crocuta* from the Museum of Natural History Vienna. Virtual endocast of sinal cavities and photo of actual skull in dorsal (left) and lateral (right) view.

is complete. After a quarter circle up from the Inion, the sagittal crest runs nearly straight to the Bregma. From there it arcs down towards the Prosthion, again with a slight disturbance at the position of the nasal bone.

The virtual endocast seems very slim in dorsal view, with very view fillings of the left and right processus zygomaticus. In lateral view the endocast is not pointed at its distal end, but reaches slightly into the crista dorsalis.

The scan was made at the University of Veterinary Medicine and consists of 76 slices at 512×512 pixels each. Each voxel has a real size of 0.586×0.586×1mm. The scan was made in sagittal view, the average HMH was 900.

4.1.12 Specimen No. 6062

The specimen is from the Museum of Natural History Vienna. It retains all its teeth and is only missing parts of its nasal bone. It was the first skull scanned at the University of Veterinary Medicine, and therefore was scanned completely with its left and right jugular bone, but on the other hand is missing some millimeters at its oral and aboral end. Because of this some distances on the skull had to be measured by conventional methods. I used a digital sliding caliper for the measurements, and ignored all but the first decimal place. For the deviation and mean compared to the CT measurements see chapter 5. These distances include Prosthion-Spina nasalis posterior distance, Prosthion-Nasion distance, Opisthion-
indexInionInion distance, Inion-Bregma distance and Inion-Prosthion distance. See also table 4.2. The Inion-Prosthion distance has been measured at 247.4mm which indicates a fairly small specimen. The skull has a very small sagittal crest. It spans along the median sagittal plain in a smooth arc towards the Nasion. There it arcs up slightly along the nasal bone, and back down again to the Prosthion. Some of the skull-sutures are still very visible.

This specimens virtual endocast of the sinal cavities looks very compact and large, nearly without the usual outcrops for the processi zygomatici. In lateral view the distal end of the endocast is well rounded.

The scan was made at the University of Veterinary Medicine and consists of 238 slices at 512×512 pixels each. Each voxel has a real size of 0.488×0.488×1mm. The scan was made in coronal view, the average HMH was 850.

4.1.13 Specimen No. 6063

This skull is from the collection of the Museum of Natural History in Vienna. It is missing none of its teeth, but part of the right canine is broken. Otherwise the skull is undamaged. Its length from Inion to Prosthion is 265.22mm. The sagittal crest arcs up from the Inion along the median sagittal plain, and goes past the Bregma in a very flat angle. Past the processi zygomatici the angle changes and goes downwards very sharply for a short distance, until reaching the Nasion, where it is reversed again along the nasal bone. From there it falls down very steeply again towards the Prosthion.
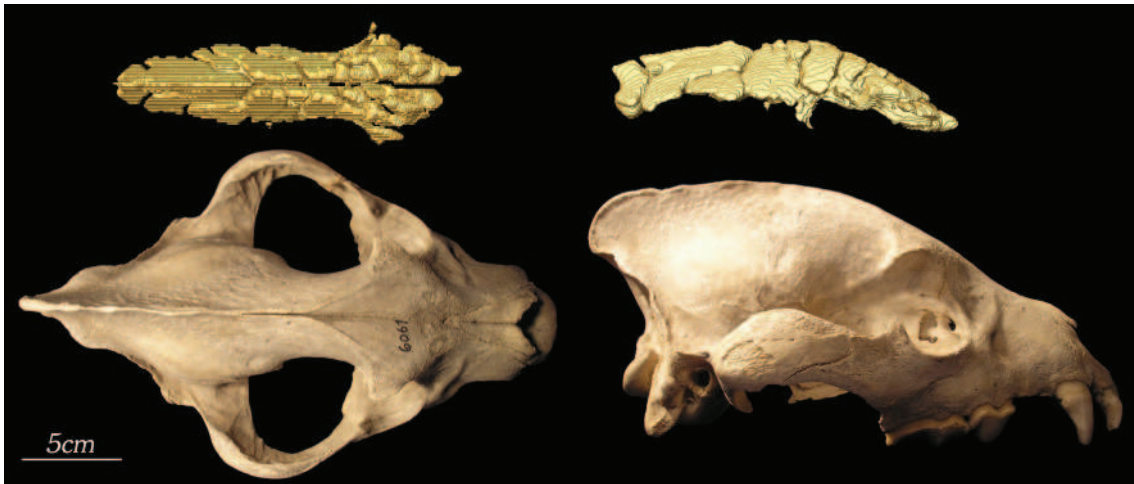
Figure 4.11: Specimen No. 6061, *Crocuta crocuta crocuta* from the Museum of Natural History Vienna. Virtual endocast of sinal cavities and photo of actual skull in dorsal (left) and lateral (right) view.

Figure 4.12: Specimen No. 6062, *Crocuta crocuta crocuta* from the Museum of Natural History Vienna. Virtual endocast of sinal cavities and photo of actual skull in dorsal (left) and lateral (right) view.

In dorsal view the virtual endocast is very asymmetric at its distal end favouring the right hemisphere. Both processi zygomatici are nearly similar filled. In lateral view it is obvious that the crista dorsalis is not filled with the virtual endocast.

The scan was made at the University of Veterinary Medicine and consists of 83 slices at 512×512 pixels each. Each voxel has a real size of 0.586×0.586×1mm. The scan was made in sagittal view, the average HMH was 780.

4.1.14 Specimen No. 6064

The specimen is from the Museum of Natural History in Vienna. It is only missing its left I[1]. The Inion-Prosthion distance was measured at 258.27mm. Beginning at the well developed beak for the Inion, the sagittal crest arcs in a steady angle forward. At the Nasion the angle is reversed a bit along the nasal bone, and then falls back down again to the Prosthion.

In dorsal view the left hemisphere of the virtual endocast of the sinal cavities is larger developed at its distal end. Many outcrops are also visible and there is a huge separation from left and right hemisphere beginning at the proximal end of the endocast and reaching halfway through it.

The scan was made at the University of Veterinary Medicine and consists of 101 slices at 512×512 pixels each. Each voxel has a real size of 0.586×0.586×1mm. The scan was made in sagittal view, the average HMH was 800.

4.1.15 Specimen No. 6617

The specimen is from the collection of the Löwentormuseum in Stuttgart. Because it was on display, it could not be removed for very long, so it was scanned on location at the Katharinenhospital in Stuttgart. It is in very good shape for a fossil, with a completely undamaged cranial and frontal region. Both zygomatic arches have not been conserved and have been restored at the museum. It is also missing its right I[2] and its left I[1-3] but retains all other teeth, which look well used and indicate long life. There is also some minor damage on the left and right bulla auditoria. The distance from Inion to Prosthion is 284,86mm. The sagittal crest is quite large. The Inion can only be positioned where the two *liniae nuchae superiores* join, because there is no beak developed at its position. From there the sagittal crest angles up along the median sagittal plain, and then down at the Bregma and past the Nasion towards the Prosthion. The nasal bone extrude just slightly from this arc.

The virtual endocast of both nasal and frontal sinus looks very small compared to the size of the specimens skull. It is well developed favouring the right hemisphere at its proximal end.

The scan consists of 260 slices at 512×373 pixels each. Each voxel has a real size of 0.402×0.402×1.25mm. The scan was made in coronal view, the average HMH was 2110.

It was not possible to identify the location Ketsch, Krenzwiese which is—according to the identification card—the place of origin of this specimen.
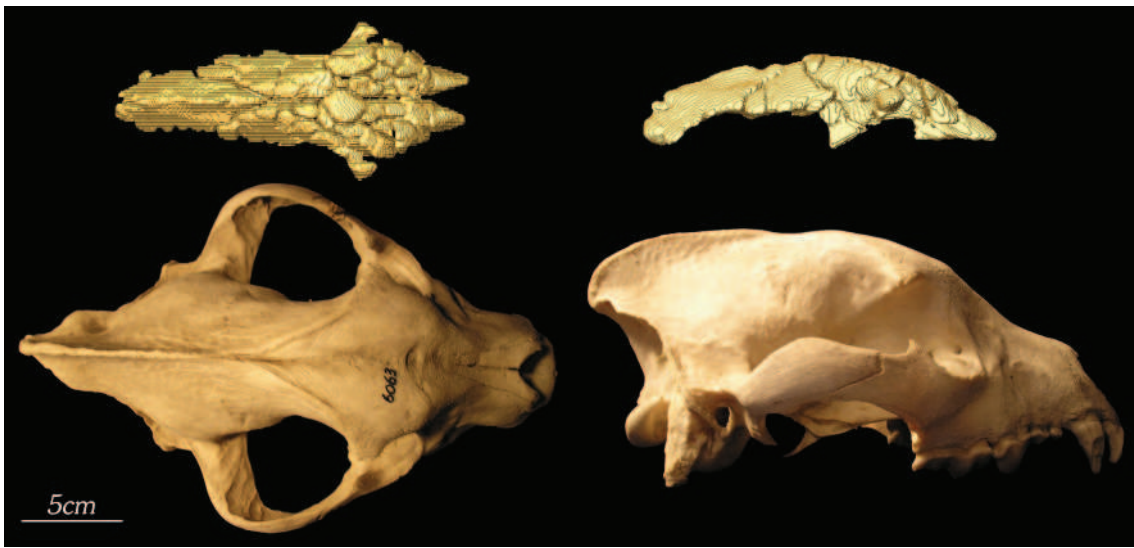
Figure 4.13: Specimen No. 6063, *Crocuta crocuta crocuta* from the Museum of Natural History Vienna. Virtual endocast of sinal cavities and photo of actual skull in dorsal (left) and lateral (right) view.
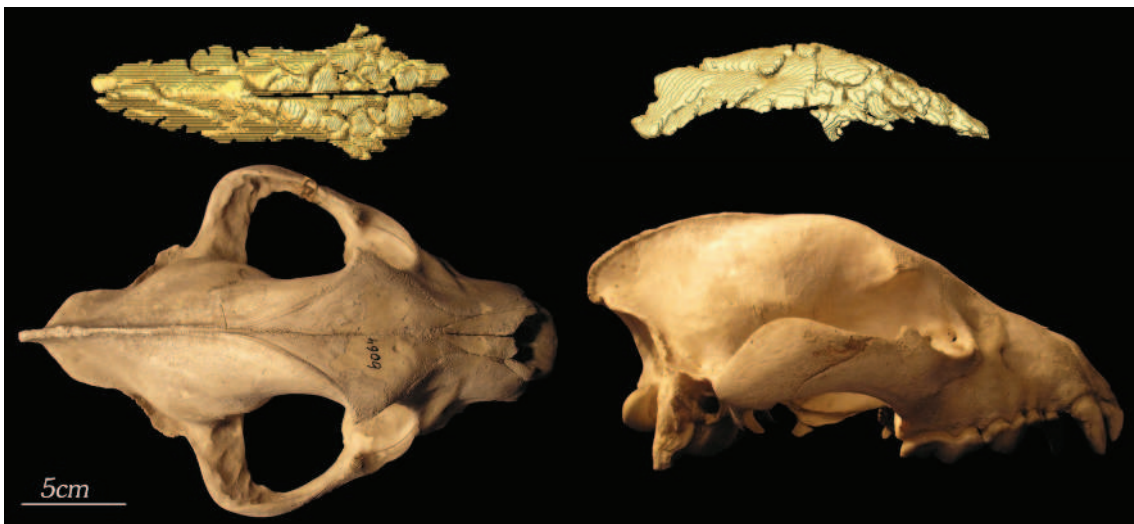

Figure 4.14: Specimen No. 6064, *Crocuta crocuta crocuta* from the Museum of Natural History Vienna. Virtual endocast of sinal cavities and photo of actual skull in dorsal (left) and lateral (right) view.

4.1.16 Specimen No. 7393

The skull is from the Museum of Natural History in Vienna. It is missing its left and right P^1, but is otherwise complete. The Inion-Prosthion distance was measured with 265.43mm which indicates an average specimen. From the beak indicating the position of the Inion, the sagittal crest is built in a single arc along the median sagittal plain, which does not change direction until the Nasion. Along the nasal bone, it changes its angle as usual a little bit, and afterwards smoothly continues down to the Prosthion.

This specimens virtual endocast is small and long in dorsal view, with nearly no striking development of the processi zygomatici (but they are also not very prominent in the real skull, compared to other specimens). In lateral view a little intrusion of the endocast into the crista dorsalis can be seen.

The scan was made at the University of Veterinary Medicine and consists of 101 slices at 512×512 pixels each. Each voxel has a real size of 0.586×0.586×1mm. The scan was made in sagittal view, the average HMH was 930.

4.1.17 Specimen No. 7397

This specimen is from the collection of the Museum of Natural History in Vienna. The skull has lost its I^{1-3} and P^4 on the right, and I^1, I^3, C^{sup} and P^{1-2} on the left side of the skull. Furthermore it has a small hole in the right bulla auditoria. Starting at the Inion, the sagittal crest angles along the median sagittal plain in a flat arc, about halfway between Bregma and Nasion it is nearly straight down to the Prosthion. Only the nasal bone extrudes a little bit from this straight line.

In dorsal view the virtual endocast is cone-shaped towards the distal end. It is very broad at the location of the frontal bone, with prominent fillings of the left and right processus zygomaticus. In lateral view it has a nice crescent shape, with a little pointed tip at its distal end.

The scan was made at the University of Veterinary Medicine and consists of 90 slices at 512×512 pixels each. Each voxel has a real size of 0.586×0.586×1mm. The scan was made in sagittal view, the average HMH was 890.

4.1.18 Specimen No. 7801

The fossil specimen is from the Löwentormuseum in Stuttgart. It is heavily damaged but with a relatively intact cranial region. It is missing most of the os incissivum along with all incisors, only retaining the alveolus of the right I^3. Along with that, there is also no Prosthion any more. It furthermore has a large hole in the cranial region of the left frontal and parietal bone. It also has major damage to its left and right sphenoidal and palatinal bones. Finally both zygomatic arches have been restored because they have not been conserved. The Inion is located at a very large beak at the dorsal side of the skull. From there the sagittal crest arcs up very smoothly to the Bregma, and then down fairly steeply past the Nasion, angling up again a little bit along the nasal bone, and then down again to the missing Prosthion. Due to the missing os incissivum the overall length of the skull can only be guessed, but has surely to be larger than 275mm.
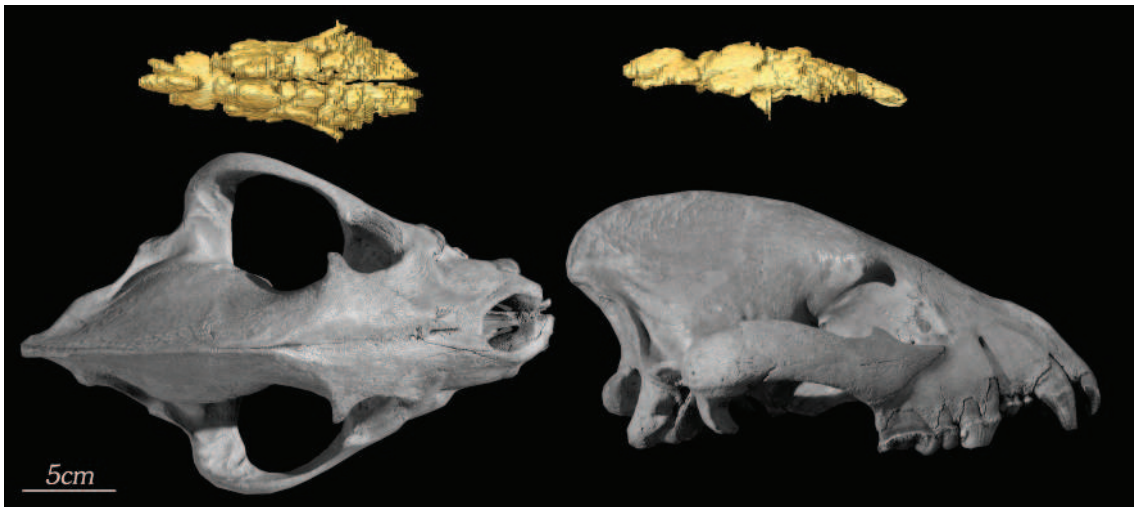
Figure 4.15: Specimen No. 6617, *Crocuta crocuta spelaea* from the Löwentormuseum in Stuttgart. Virtual endocast of sinal cavities and photo of actual skull in dorsal (left) and lateral (right) view.

Figure 4.16: Specimen No. 7393, *Crocuta crocuta crocuta* from the Museum of Natural History Vienna. Virtual endocast of sinal cavities and photo of actual skull in dorsal (left) and lateral (right) view.

The damage to this specimen made the usual technique impracticable, because both cavities I had to measure were missing some limits. Therefore I only measured the right half of the skull up to the median sagittal plain (which was easy to identify because of the differentiation between the left and right lobe of the sinus frontalis). I then simply doubled the volume data to simulate the complete cavities.

Due to the fragmentation of the skull the actual virtual endocast consists only of the right hemisphere. Therefore no comparism of the asymmetry can be given. Nevertheless the right processus zygomaticus is well filled with the endocast.

The scan was made at the University of Veterinary Medicine and consists of 86 slices at 512×512 pixels each. Each voxel has a real size of $0.684 \times 0.684 \times 1$mm. The scan was made in sagittal view, the average HMH was 900.

The Irpfelhöhle near Giengen an der Brenz gets a short description in Andree (1939) mainly concerning its anthropological findings of stone craftsmanship. But there is also a brief listing of its fauna included.

4.1.19 Specimen No. 19062

The specimen is also a fossil from the Löwentormuseum in Stuttgart. It is also heavily damaged but luckily it was—even with greater damage than specimen 7801—more complete in its cranial region and therefore easier to measure. It is missing its right I^1 and left I^{1-2}. It is also missing its right P^{3-4} along with most of its right maxillary and frontal bone. The damage also includes the missing right sphenoidal and palatinal bone and most of the interior of the nose. Also its complete secondary palatinum is missing along with the Spina nasalis posterior. Both bullae auditoriae have large holes too. Finally the nasal bone and the left zygomatic arch have been rebuilt. Luckily the damage on the inside of the skull is not even reaching the median sagittal plain, and therefore at least the left half of the skull could be measured without any problems. To get the best results, I started measuring the complete left hemisphere of the sinal cavities and doubled the result for the final data. Additionally, I afterwards measured the complete part of the sinal cavities that overlies the endocranium, and then additionally measured the left half of the sinus frontalis. By doubling the data from the sinus frontalis, and adding the part from above the endocranium, I also got the complete volume data for the sinal cavities. I took the mean value of both generated volumes to produce the most realistic volume data for the sinal cavities, which is now used in the results table. The endocranial cavity was luckily complete, only missing a small part of the olfactory bulb. Therefore I took a similar approach, first measuring the left hemisphere of the endocranial cavity, doubling the volume-data at the end. Then I measured the complete endocranial cavity, completing the small missing part. Again I took the mean of both measurements to get the final volume data used in the results table. For measuring the length of the skull the usual distance from Prosthion to Inion was used. The distance indicates at 266.78mm only an average skull.

Similar to specimen 7801, parts of the virtual endocast of this specimen had to be added digitally. As to my description above only the part around the right nasal and frontal bone had to be computed this way. The actual (real) parts of the sinal cavities
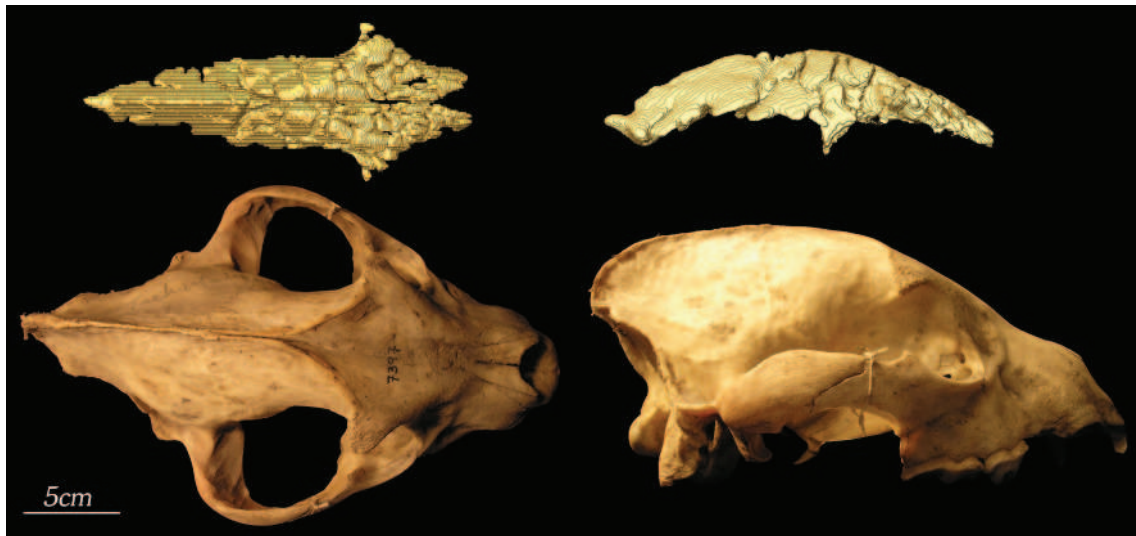
Figure 4.17: Specimen No. 7397, *Crocuta crocuta crocuta* from the Museum of Natural History Vienna. Virtual endocast of sinal cavities and photo of actual skull in dorsal (left) and lateral (right) view.
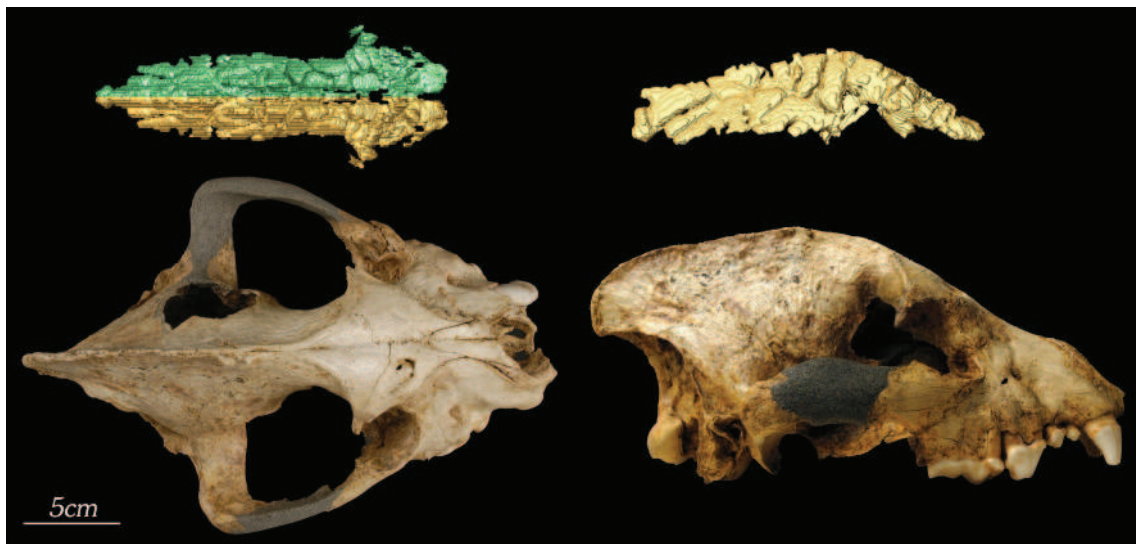

Figure 4.18: Specimen No. 7801, *Crocuta crocuta spelaea* from the Löwentormuseum in Stuttgart. Virtual endocast of sinal cavities and photo of actual skull in dorsal (left) and lateral (right) view. Displayed in green on the virtual endocast is the digitally completed nasal and frontal sinus.

are well developed, especially at the distal end where the endocast reaches far into the crista dorsalis (in lateral view). In dorsal view the distal end is cone-shaped.

The scan was made at the University of Veterinary Medicine and consists of 103 slices at 512×512 pixels each. Each voxel has a real size of 0.625×0.625×1mm. The scan was made in sagittal view, the average HMH was 960.

The place of origin of this specimen could not be verified, because around the village of Erkenbrechtsweiler where it was found according to its identification-card, there are a multitude of possible locations.

4.1.20 Specimen No. 21495

The skull is from the collection of the Museum of Natural History in Vienna. It is missing its left C^{sup} and P^2 and its right I^3. There is also a very small hole in the left bulla auditoria and some parts of the left and right nasal bone are missing. The distance from Inion to Prosthion is about 266.68mm which indicates an average individual. The Inion is only recognizable at the crosspoint of the two *liniae nuchae superiores* because there is no beak developed at its position. From there, the sagittal crest has the typical arc along the median sagittal plain forward to the Prosthion. The nasal bone disturbs this smooth arc a little bit, but just slightly.

The virtual endocast of the sinal cavities is cone-shaped in dorsal view, and crescent-shaped in lateral view. At its distal end, a small pointed tip thrusts upward into the crista dorsalis. In dorsal view the parts around the frontal bone are very broad and compact developed.

The scan was made at the University of Veterinary Medicine and consists of 79 slices at 512×512 pixels each. Each voxel has a real size of 0.586×0.586×1mm. The scan was made in sagittal view, the average HMH was 900.

4.1.21 Specimen No. III

The specimen is from the collection of the Krahuletz-Museum in Eggenburg. The cranial skull itself is mostly complete, but is missing both zygomatic arches because they have not been conserved. The skull is also missing its left and right P^1, canines and all incisors, but retains the left and right P^{2-4}. Furthermore the nasal bone is missing some parts on its left and right side, and half of the left bulla auditoria is missing too. The right bulla auditoria has only a small hole.

The virtual endocast is fairly large with well accentuated lobes along its whole body. In lateral view it is very high, reaching far into the crista dorsalis. At its distal end it is very wide developed.

The CT-scan was made at the Universitätsklinik Innsbruck in the year 2002 by the Department of Anthropology of the University of Vienna, but the acquired data has not been used in any publication since then, except a poster at the 12th RCMNS conference in Vienna, Autumn 2005. The scan consists of the whole skull. It consists of 194 slices at 512×512 pixels each. Each voxel has a real size of 0.594×0.594×1mm. The scan was made in transverse view, the average HMH was 750.

Figure 4.19: Specimen No. 19062, *Crocuta crocuta spelaea* from the Löwentormuseum in Stuttgart. Virtual endocast of sinal cavities and photo of actual skull in dorsal (left) and lateral (right) view. Displayed in green on the virtual endocast is the digitally completed nasal sinus.
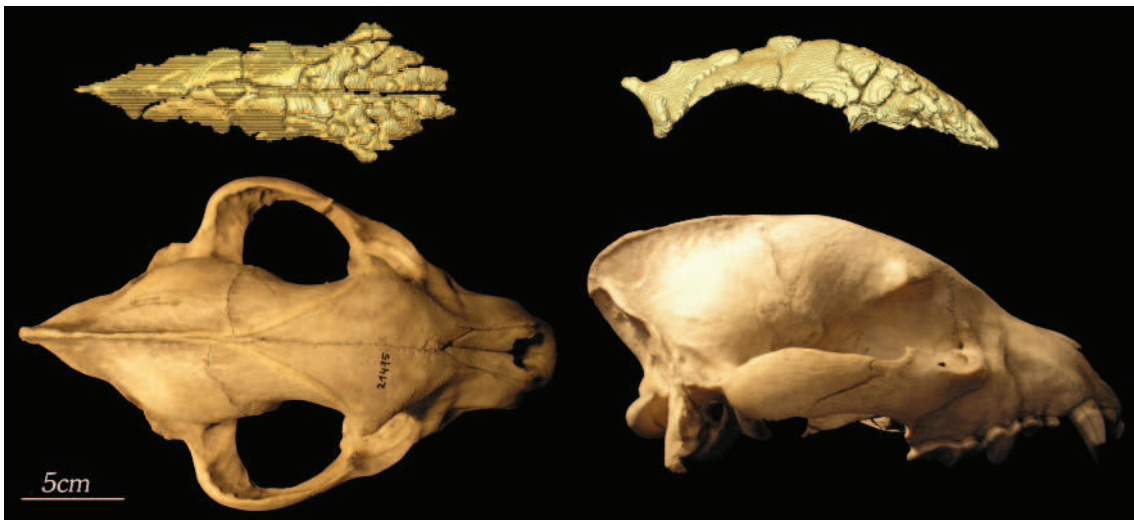

Figure 4.20: Specimen No. 21495, *Crocuta crocuta crocuta* from the Museum of Natural History Vienna. Virtual endocast of sinal cavities and photo of actual skull in dorsal (left) and lateral (right) view.

The specimen number III from the Krahuletz-Museum in Eggenburg was described by Ehrenberg et al. (1938). It was found in a cave located northeast of Eggenburg (Lower Austria) on the northern slope of the Königsberg. This cave is called "Fuchslucken", "Fuchsloch" or "Teufelslucken" by the locals. The sedimentary basis is crystalline and is composed of granites and gneiss upon which is a thin Neogene layer (Burdigal). The Neogene sediments consist of two different compositions; one is a compact, banked sandstone in the

Those loose sands have been gradually removed by erosion and between the sandstone and basal crystalline the cave came into existence. At the time of the colonization, the development of the cave was completed. Through continuing erosion the size of the cave was reduced by back-setting of the entrance.

If local tales can be believed the cave was full of bones in the early years of the 19th century but periodical robbery reduced the fossil material and anthropogene artifacts to a minimum when Johann Krahuletz made his excavations from 1887 to 1889.

The complete specimens found in the Teufelslucken until today are assumed to be less than half of the original richness of the cave in early 1800.

4.1.22 Specimen No. IPB M 432

The specimen is from the Goldfuß-Museum in Bonn. It is missing its I^1 and P^1, and its left I$^{1\text{-}2}$ and C^{sup}. It also has a broken left and right bulla auditoria, and part of its right linia nucha superioris is missing up to the median sagittal plain, therefore the Inion is only identifiable through the crosspoint of the left linia nucha superioris with the median sagittal plain, which is because of the damage a little out of place to the left side of the skull. Also the sagittal crest has lost most of its dorsal part to the damage. The Inion-Prosthion distance was measured at 266.97mm. Beginning at the broken part of the sagittal crest, it arcs along the median sagittal plain very smoothly towards the Prosthion, with not as much as a disturbance along the nasal bone. In sagittal view, the skull looks very straightforward and streamlined.

The virtual endocast of the sinal cavities is very flat in lateral view matching the actual skull-shape very well. It is however not very broad in dorsal view, and with nearly no fillings of the left and right processus zygomaticus. The whole endocast looks small compared to the skull of the specimen.

The scan was made at the University of Veterinary Medicine and consists of 99 slices at 512×512 pixels each. Each voxel has a real size of 0.586×0.586×1mm. The scan was made in sagittal view, the average HMH was 1490.

This specimen has not been reviewed until now, but its place of discovery is the famous Zoolithenhöhle near Burggaillenreuth in Franconia. The cave has been known by locals since the 17th century for its rich fauna. The first complete review was written by Johann Friedrich Esper (Esper, 1774) who was the pastor in Uttenreuth and also was very interested in the natural sciences. In the years between 1771 and 1774, he made extensive excursions to the cave to recover many bones found there, and describe the cave itself. According to him, all of the bones were embedded in cave clay and many were coated with sinter. Since then the cave has been revisited many times and much

material has been recovered. Georg August Goldfuss made detailed reviews of many of the specimens, and reviews a different cave hyena in Goldfuss (1823, pg. 451–562). A complete layout plan of the cave was published by Neischl (1903, 1904) who classifies the cave as a karst cave built in the young Tertiary period[1]. The rock itself dates back to the Malm epoch (precisely Malm delta to epsilon[2]) (Neischl, 1903, 1904). The last palaeontological excavation was made in 1971 and a complete report can be found in Heller (1972). Since this time the cave has been closed to the public to prevent further fossil robbing, which occurred very often before.

4.2 Measurements of Specimens

For this study different information has been gathered about the 22 specimens. The digital fillings of the endocranial cavities and the nasal sinuses produced volume data which is summed up in table 4.1. Additionally some distances between exactly defined points on the skull have been measured on the digital data-sets of the specimens. This information is given in table 4.2. The exact definition of the different measuring points chosen for this is shown below, along with a schematic (figure 4.23).

Basion This point lies where the frontal edge of the *foramen magnum* intersects with the median sagittal plain. It is exactly opposite the *Opisthion*.

Bregma cf The actual *Bregma* is the crosspoint between the left and right parietal bone and left and right frontal bone. Because it was not possible to see the bone fissures in the CT-scans, I defined the *Bregma cf* as the point where the left and right arcs of the *pars temporalis* of the frontal bone merge.

Inion This point is defined on the median sagittal plain where the two *liniae nuchae superiores* merge, which is very often visible in transverse view as a beak at the occipital part of the sagittal crest.

Nasion This point is defined as the crosspoint between the left and right frontal bone and the left and right nasal bone.[3]

Opisthion This point lies where the back edge of the *foramen magnum* intersects with the median sagittal plain. It is exactly opposite the *Basion*.

Prosthion This point is defined as the point on the median sagittal plain which lies in the exact centre between the two I[1].

---

[1]Neogene

[2]middle to upper Kimmeridge

[3]It was sometimes hard to actually find this point in the CT-scans, because of obliteration of the sutures in mature or senile specimens. But by using photographs and different thresholds for the air/bone limit when rendering a 3D-reconstruction in *Amira* it was nearly always possible to exactly define it. The only exception is specimen 7397, where the actual *Nasion* is defined as *Nasion cf* at the centre point of the coadunate area.
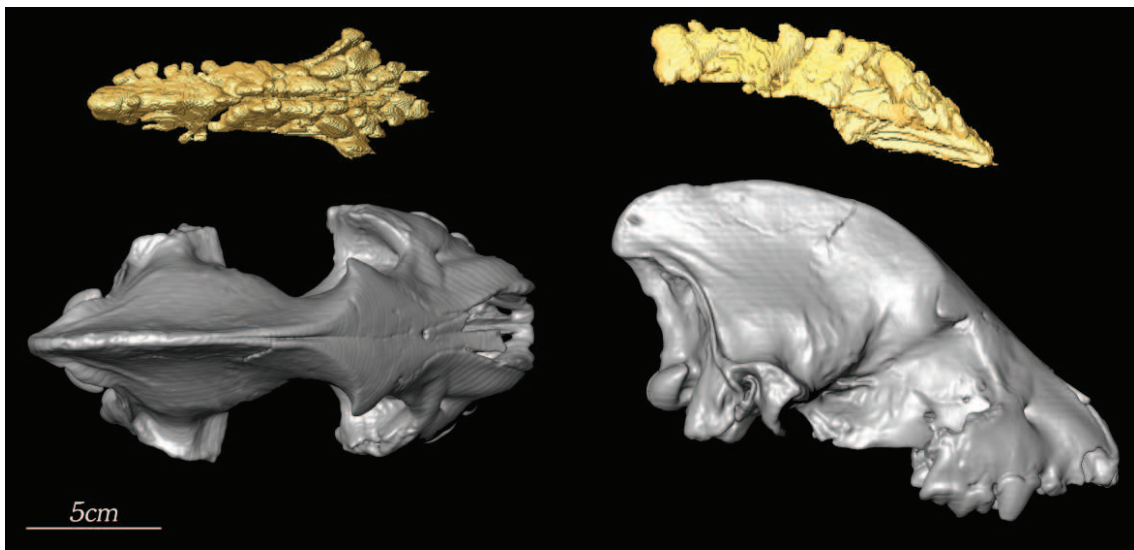
Figure 4.21: Specimen No. III, *Crocuta crocuta spelaea* from the Krahuletz-Museum in Eggenburg. Virtual endocast of sinal cavities and digital reconstruction of actual skull in dorsal (left) and lateral (right) view.
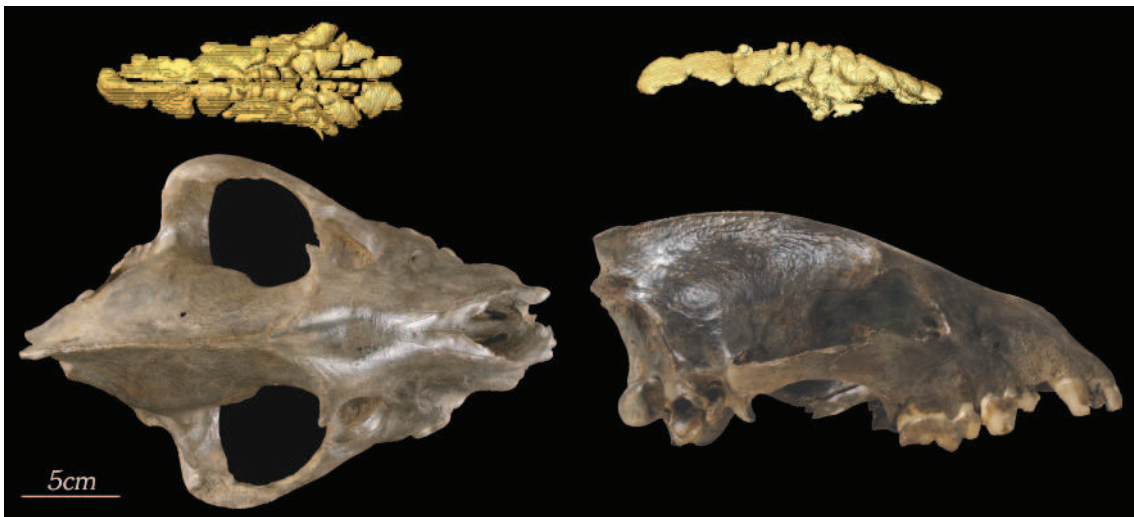

Figure 4.22: Specimen No. IPB M 432, *Crocuta crocuta spelaea* from the Goldfuß-Museum in Bonn. Virtual endocast of sinal cavities and photo of actual skull in dorsal (left) and lateral (right) view.

Spina nasalis posterior This point is the most aboral point of the secondary palatum along the median sagittal plain.

C-C distance The distance between the innermost (palatinal) points of both Canines.

P^4-P^4 distance The distance between the innermost (palatinal) points of both P^4. This point is located exactly at the outer rim of the tooth near the *Protocone*.
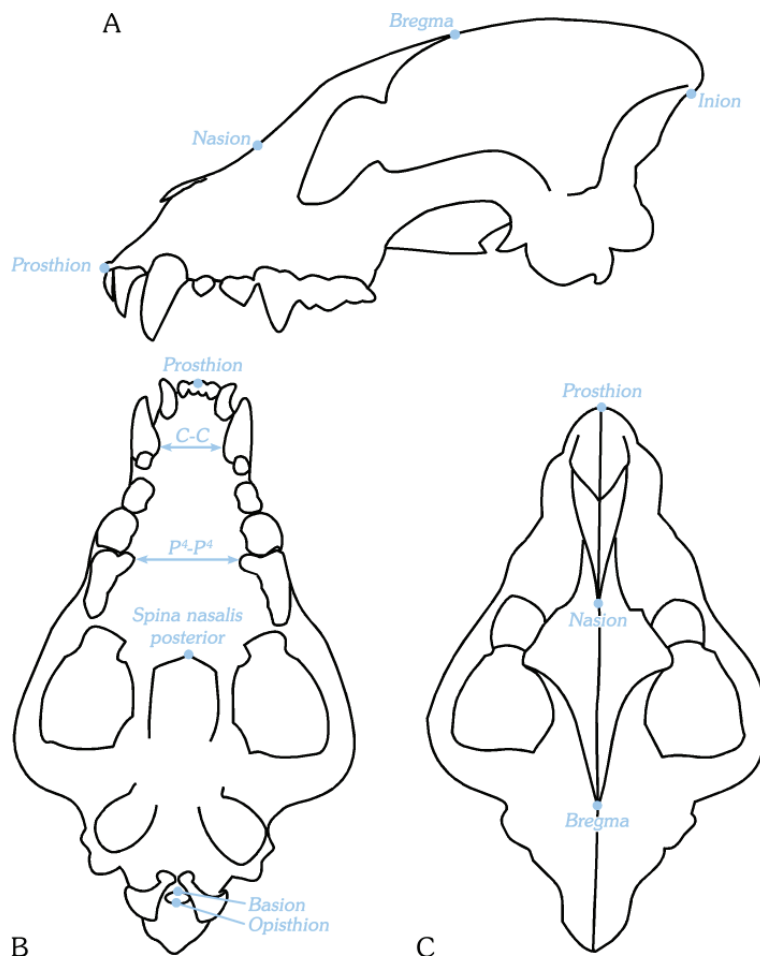
Figure 4.23: Schematic of the points used for measuring. A - lateral view, B - ventral view, C - dorsal view.

No.	Specimen type	Sinal cavity volume (mm^3)	Cranial capacity (mm^3)	% Cranial capacity to sinal volume
397	*Crocuta crocuta crocuta*	108456.65	203942.97	65.3%
1150	*Crocuta crocuta crocuta*	99331.00	180327.84	64.5%
1244	*Crocuta crocuta crocuta*	63025.24	191262.69	75.2%
1373	*Crocuta crocuta crocuta*	69142.70	182972.60	72.6%
1755	*Crocuta crocuta crocuta*	74035.62	163473.41	68.8%
1756	*Hyaena hyaena*	69232.52	112030.53	61.8%
2531	*Hyaena hyaena*	82930.44	110287.13	57.1%
3919	*Crocuta crocuta crocuta*	85882.34	190995.58	69.0%
5584	*Crocuta crocuta crocuta*	132785.11	191154.88	59.0%
6061	*Crocuta crocuta crocuta*	82194.35	163613.83	66.6%
6062	*Crocuta crocuta crocuta*	82090.77	173900.43	67.9%
6063	*Crocuta crocuta crocuta*	112528.69	183000.27	61.9%
6064	*Crocuta crocuta crocuta*	95269.48	165918.21	63.5%
6617	*Crocuta crocuta spelaea*	63738.70	199321.88	75.8%
7393	*Crocuta crocuta crocuta*	74429.75	194770.08	72.4%
7397	*Crocuta crocuta crocuta*	123259.61	220436.24	64.1%
7801	*Crocuta crocuta spelaea*	116566.30	201947.76	63.4%
19062	*Crocuta crocuta spelaea*	91950.00	205040.05	69.0%
21459	*Crocuta crocuta crocuta*	106577.52	197151.37	64.9%
1744/B	*Crocuta crocuta crocuta*	185099.70	180513.61	49.4%
III	*Crocuta crocuta spelaea*	128186.38	201892.42	61.2%
IPB M 432	*Crocuta crocuta spelaea*	53339.40	213835.17	80.0%

Table 4.1: Volume data from the nasal sinuses and the endocranium of the measured specimens.

No	Specimen type	Palatum	Snp-Ba	Ba-Op	Op-In	In-Br	Br-Na	Na-Po	Skull	C-C	P^4-P^4
397	*C. crocuta crocuta*	138.08	109.27	23.38	46.07	130.04	81.02	111.92	287.18	42.79	70.43
1150	*C. crocuta crocuta*	120.81	na	na	na	95.21	92.59	91.45	252.16	37.12	61.70
1244	*C. crocuta crocuta*	131.41	95.51	23.09	49.16	130.97	63.43	100.40	267.73	na	69.55
1373	*C. crocuta crocuta*	103.01	103.63	25.29	37.68	95.64	83.15	90.13	237.14	34.78	52.98
1755	*C. crocuta crocuta*	119.24	96.93	19.47	45.50	125.84	62.30	101.67	256.69	33.25	58.50
1756	*H. hyaena*	107.54	91.15	19.13	30.95	76.61	100.51	74.67	223.80	29.56	46.37
2531	*H. hyaena*	114.53	88.12	19.59	37.57	98.63	85.24	68.21	233.03	28.36	54.95
3919	*C. crocuta crocuta*	117.18	100.96	23.56	41.55	103.59	83.71	92.56	247.70	34.35	61.25
5584	*C. crocuta crocuta*	131.32	118.79	26.51	44.27	110.70	117.45	102.38	291.17	43.26	69.30
6061	*C. crocuta crocuta*	119.15	109.57	26.81	50.72	128.63	69.48	102.49	272.80	37.30	58.18
6062	*C. crocuta crocuta*	*118.8*	95.93	22.46	*40.9*	*76.4*	96.38	*92.7*	*247.4*	32.26	58.21
6063	*C. crocuta crocuta*	124.57	101.08	23.18	45.22	99.94	100.09	97.65	265.22	37.94	60.48
6064	*C. crocuta crocuta*	119.62	99.78	21.47	45.27	105.17	98.49	88.69	258.27	38.16	61.99
6617	*C. crocuta spelaea*	138.08	104.13	25.26	51.93	128.29	85.91	98.88	284.86	37.92	73.21
7393	*C. crocuta crocuta*	125.41	93.79	24.78	49.44	129.85	74.51	92.13	265.43	34.94	56.72
7397	*C. crocuta crocuta*	123.63	112.57	25.66	52.44	124.53	94.62	97.23	281.17	38.44	66.77
7801	*C. crocuta spelaea*	na	109.44	22.14	51.27	145.68	72.22	na	275+	46.09	79.02
19062	*C. crocuta spelaea*	na	na	22.45	47.51	125.45	na	na	266.78	42.35	na
21459	*C. crocuta crocuta*	123.60	97.41	24.32	50.67	96.55	99.22	102.05	266.68	35.08	61.54
1744/B	*C. crocuta crocuta*	131.27	108.42	22.21	55.08	116.82	102.52	105.16	288.03	41.72	64.39
III	*C. crocuta spelaea*	na	109.65	23.97	57.20	108.48	122.09	na	283+	na	78.87
IPB M 432	*C. crocuta spelaea*	124.59	104.58	24.05	49.33	117.56	68.43	109.21	266.97	40.72	71.22

Table 4.2: Distances and length data from different points located on the skull of the measured specimens. *Distances:* Palatum = Prosthion to Spina nasalis posterior, Snp-Ba = Spina nasalis posterior to Basion, Ba-Op = Basion to Opisthion, Op-In = Opisthion to Inion, In-Br = Inion to Bregma cf, Br-Na = Bregma cf to Nasion, Na-Po - Nasion to Prosthion, Skull = Inion to Prosthion, C-C = innermost canine distance, P^4-P^4 = innermost P^4 distance. *Italic* data indicates measurements with traditional methods; see text for further details.

5 Applied Statistics

5.1 Reliability of Measurements

For reliability of the measurements, I compared digital distance measuring with conventional distance measuring methods. Therefore I used the Inion-Bregma distance of specimen No. 397. I measured the distance digitally in two ways, once by defining landmarks, and measuring with the help of these indicators, and second without the landmarks only by morphometric features of the skull. For the conventional method I used a sliding caliper with digital display and measured the distance on the specimen according to its morphometric features. I made 10 measurements in each of the three ways to compare with each other. The results are shown in table 5.1.

	with landmarks/ conventional (result in mm)	without landmarks/ conventional (result in mm)
n	10	10
Mean	0.85	1.23
Standard Distribution	0.53	0.56
Standard Error of Mean	0.17	0.17
Median	0.82	1.19
25%	0.42	0.81
75%	1.24	1.64
Minimum	0.11	0.45
Maximum	1.71	2.12

Table 5.1: Mean and deviation of measurements. The first column displays digital measurements with landmarks compared to conventional measurements with a sliding caliper, the second column displays digital measurements without landmarks compared to conventional measurements with a sliding caliper.

The digital measurements with the CT-data were slightly larger than the conventional measurements, especially without the use of landmarks, where the data was a little more widespread. By using landmarks for relocating the measured points, the absolute difference to conventional measurements is 0.85mm ± 0.53mm. Without the help of these landmarks it grows to 1.23mm ± 0.56mm. Exactly 50% of the observations with the help of landmarks are located between 0.42mm and 1.24mm. Without using

landmarks the area itself is about the same, but shifts up a bit to between 0.81mm and 1.64mm. It seems relocating the measuring points digitally without landmarks as guidelines is more difficult and leads to larger overestimation of observations compared to the conventional method. Therefore it is crucial to keep in mind, that all the data in this study was acquired by the same means using landmarks for locating the different measuring points, and comparison to conventionally acquired data from the same specimens is not possible without adjustment of the observations.

For reliability in volume data extensive tests were done on human skulls by Weber et al. (1998) using the HMH method described in chapter 2 and conventional methods with mustard seed and water displacement. According to that study, the digital measurements underestimated the measurements by conventional methods by around 2.26% ± 0.86%. I did no comparison in volume measurement with conventional methods on my specimens, but rely on Weber et al. (1998) for the accuracy of my observations.

5.2 Comparison of Volume Data

Now, after determining the reliability of the measurements, further analysis is possible. The data used in these methods comprises of both raw and adjusted data. To make a comparison between distance data and volume data possible, the 3$^\mathrm{rd}$ root was extracted from the raw volume data, thus adjusting both data sets to the same dimension. Inside each sample group, time is not an important factor, as each group comprises of specimens from the same time level. All the *Crocuta crocuta crocuta* and *Hyaena hyaena* specimens are from recent times, and all the *Crocuta crocuta spelaea* specimens are about the same age, dating back around 30 000 years. The specimens are also from about the same altitude, as none of them were living in the high mountains. Therefore altitude reaches from sea level to a maximum of 2 000m.

To compare the sinal and cranial volume data with conventional statistical methods, it was first important to check for a normal distribution of the observations. This was verified through the Kolmogorov-Smirnov-Test by means of the largest sample group of *Crocuta crocuta crocuta*. According to this, also the smaller sample groups of *Crocuta crocuta spelaea* and *Hyaena hyaena* are assumed to have normal distribution.

The distribution of the sinal and cranial volume data compared to the skull length is given in figures 5.1, 5.2, 5.3 and 5.4. Because of missing exact skull length in specimens 7801 and III, it is important that the measured distance from table 4.2 was not altered and thus the data used is underestimating the original skull size. Additionally, to get a linear ascent instead of an exponential ascent, the 3$^\mathrm{rd}$ root was extracted from the volume data as mentioned above.

When looking the diagram in figures 5.1 and 5.2, the measuring point for specimen 1744/B seems to be an out-lier to the rest of the sample. Through a t-Test for determining outliers (Elser, 2004), this impression was verified.

Comparison of the sinal volume data through a t-Test (Elser, 2004), with adjusted data by extracting the 3$^\mathrm{rd}$ root, confirms that *Crocuta crocuta crocuta* and *Crocuta crocuta spelaea* belong to the same basic population. The 95% confidence interval for

	C. c. crocuta	*C. c. spelaea*	*H. hyaena*
f(x)	5.7535x	6.1305x	5.3938x
R^2	-0.3634	-13.645	0.7613

Table 5.2: The slope for the regression lines for the sinal volume.

	C. c. crocuta	*C. c. spelaea*	*H. hyaena*
f(x)	4.6604x	4.673x	4.7503x
R^2	-0.1541	-0.5478	-0.2755

Table 5.3: The slope for the regression lines for the cranial capacity.

Mean is larger for the smaller *Crocuta crocuta spelaea* sample, reaching from 39.95mm through 48.85mm. The larger *Crocuta crocuta crocuta* sample lies within this range with a 95% confidence interval for Mean of 43.37mm through 48.51mm. Due to the small sample size of *Hyaena hyaena* it takes no part in these calculations.

The regression line for each of the three samples looks very promising in terms of producing the same connection between skull length and sinal volume. Because the size of the cranial cavities is dependent on the overall skull size, the volume data is depending on the skull length as shown in the diagram. The slope of the regression lines is given in table 5.2.

I chose a regression line through the origin, because the connection between skull length and size of cavities is logically existent, but a normal regression shows different results with the smaller samples. For example the conventional regression line for the cranial capacity of *Crocuta crocuta spelaea* (see figure 5.3) would have shown the longer the skull, the smaller the brain! The sample size of *Crocuta crocuta spelaea* and especially *Hyaena hyaena* is therefore simply too small for interpretations of conventional regression.

Comparison of the cranial capacity data through a t-Test, with adjusted data by extracting the 3$^{\rm rd}$ root, shows for *Crocuta crocuta crocuta* a 95% confidence interval for Mean of 56.22mm through 57.77mm and for *Crocuta crocuta spelaea* of 57.56mm through 60.24mm. By this test, there is just a 5% confidence, that *Crocuta crocuta crocuta* and *Crocuta crocuta spelaea* belong to the same basic population.

However, the regression lines through the origin show very similar behaviour, with the measurements given in table 5.3.

Therefore another test was made to verify if cranial capacity or sinal volume are dependent on another parameter. This was achieved by usage of an F-Test (Elser, 2004) with a 95% confidence interval. Comparison of all three samples through this test increases the credibility of the t-Tests. The number of groups for the F-Test were the three animal groups measured (*Crocuta crocuta crocuta Crocuta crocuta spelaea* and *Hyaena hyaena*), the number of samples was the sum of specimens for each group. The measurements used were sinal volume and cranial capacity, each with its own F-Test.

According to the F-Test for sinal volume, with a 5% probability of error, there is no parameter influence given, and the differences in the measurements are only accidental. This can be correlated with the outcome of the t-Test for sinal volume which states all
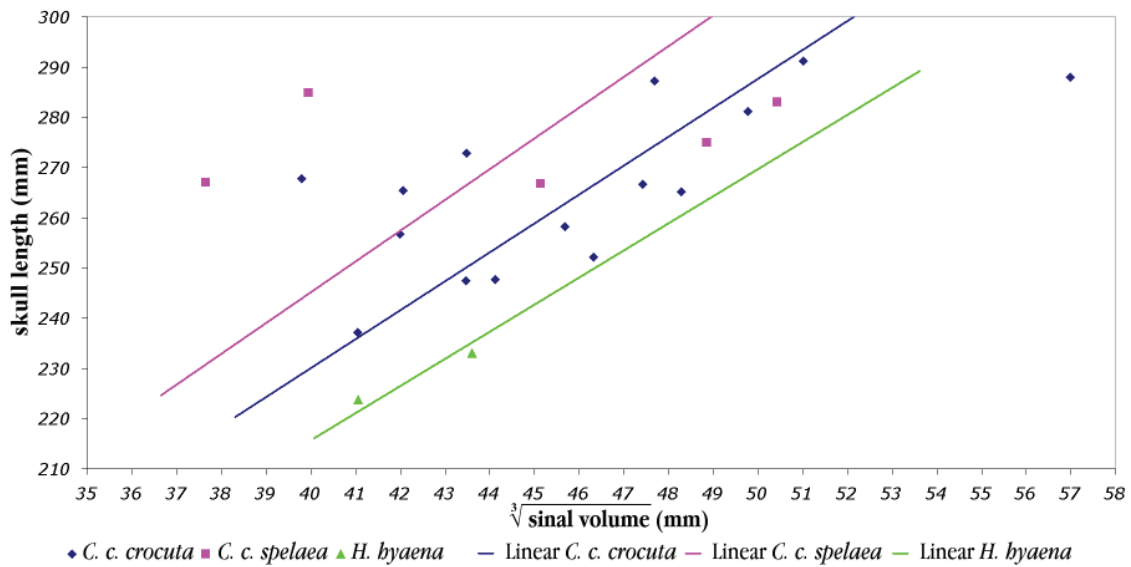
Figure 5.1: Comparison of skull length to sinal volume.
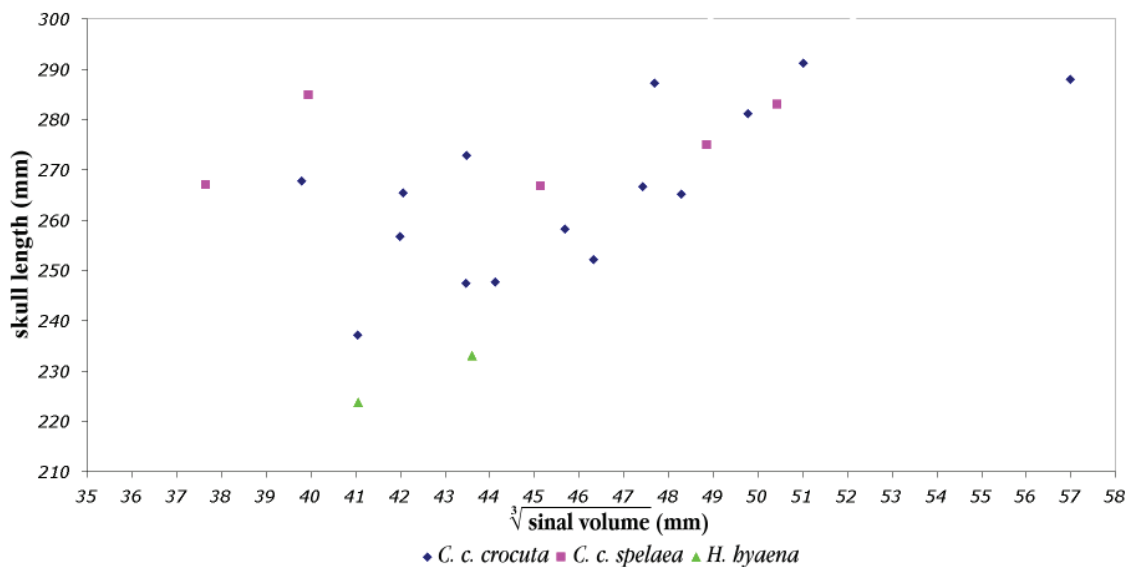
Figure 5.2: Comparison of skull length to sinal volume without regression lines.
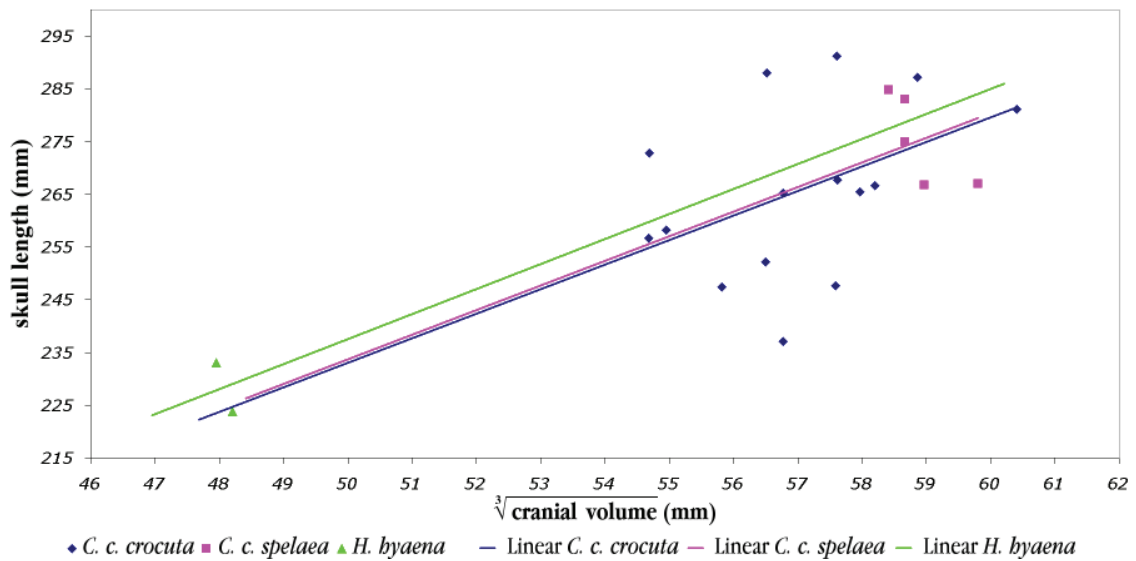
Figure 5.3: Comparison of skull length to cranial capacity with regression lines.
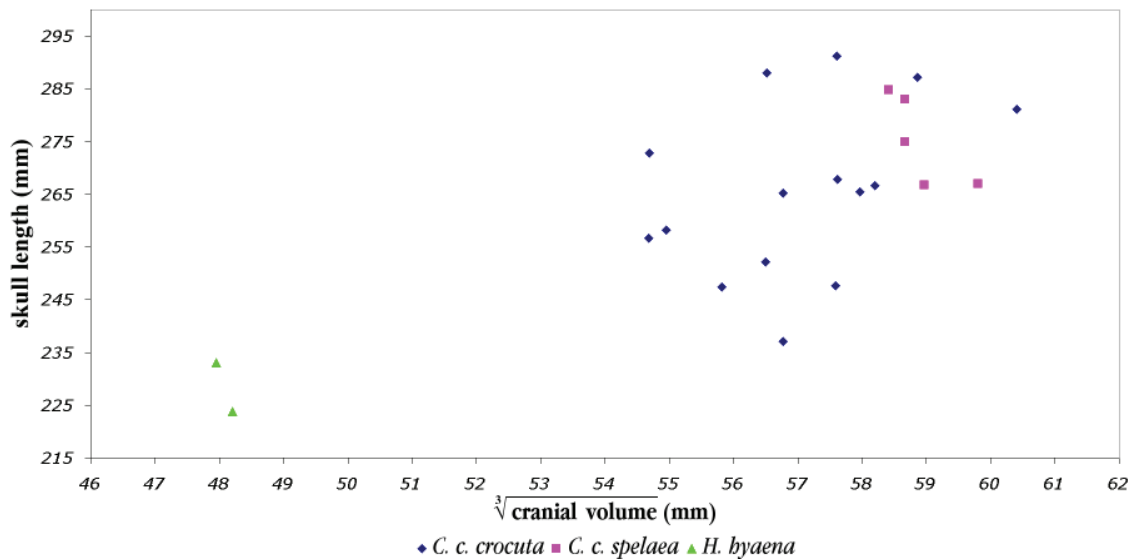

Figure 5.4: Comparison of skull length to cranial capacity without regression lines.

the sample groups belong to the same basic population.

The F-Test for cranial capacity, also with a 5% probability of error, proves a paramteter influence, and negates accidential behaviour of the measurements. This correlates with the t-Test for cranial capacity where *Crocuta crocuta crocuta* and *Crocuta crocuta spelaea* belong to different groups and not to the same basic population.

6 Discussion and Conclusion

The computer tomographic method has shown very promising results and new data could be acquired about the interior structures of precious fossil specimens where conventional methods could not be applied. Additionally new methods of visualisation are now available to show the interior of the specimens. The digital data provides permanent accessibility and the possibility of further study without the original specimen. Furthermore any research applied on the virtual object can be saved and thus reproduced exactly later. Some of the conclusions which can be drawn by now are:

The acquired data shows interesting connections between the cranial capacity and sinal volume of *Crocuta crocuta crocuta* and *Crocuta crocuta spelaea* which should be exploited further. The most interesting part is the separation of *Crocuta crocuta spelaea* from *Crocuta crocuta crocuta* through statistical analysis of the cranial capacity, whereas sinal volume data shows a clear connection between both basic populations. Through the statistical tests which were applied, a parameter-influence is visible in cranial capacity, which separates the three sample groups (altough it is not clear, which parameter is responsible, but it is possibly the skull-size). On the other hand, there is no parameter-influence but just accidental difference in the size of the sinal cavities.

If we take this into account, it was not possible to verify a distinct difference in the sinal cavities between the fossil and recent hyaenine hyaenids. The distribution of the different samples shows a lot of variation, so more samples are needed to get a better resolution. The sinal cavities of *Crocuta crocuta crocuta* and *Crocuta crocuta spelaea* belong to the same set of values, and the chance of changing that is quite small. The small sample size of *Hyaena hyaena* was only for comparison and thus is not incorporated in the conclusion.

Ignoring the measurements, even the simple design of the sinal cavity's virtual endocasts demonstrates the vast possibilities of these unusual skull traits. Limits in length and breadth are only possible by descriptive means, until measuring points and missing landmarks are defined. Additional to the measured volume data, the design of the sinal cavities is an important inspiration for further research. Comparison of these cavities with actual volume data ranges from specimens like IPB M 432, where the cranial capacity takes 80.0% of the combined cranial and sinal cavities, to specimens like 1744/B which has a larger sinal cavity than cranial capacity (49.4% of the whole cavity is cranial capacity). Outliers like 1744/B show the unexpected size possible for the sinal cavities. However two thirds of the specimens remain at 50-60% cranial capacity to sinal volume, independent of actual group association.

At this point, the author can find no difference in nasal and frontal sinus design

between *Crocuta crocuta spelaea* and the recent populations of *Crocuta crocuta crocuta* and *Hyaena hyaena*. Potentially different habitat and ecology (i.e. family life or hunting behaviour) obviously have no major influence on sinus development. The same can also be said about brain size and design, which seems to change typically with gerneral animal size.

Acknowledgments

My thanks go especially to my master thesis tutor Dr. Doris Nagel, who interpreted my general interest in computers on one side and paleontology on the other, in the right way, and gave me the inspiration for this master thesis. I want to thank my second master thesis tutor Dr. Gerhard Forstenpointner as well, for his spontaneous interest in this study and his constructive help on different matters.

The University of Veterinary Medicine Vienna (VUW), Veterinärplatz 1, A-1210 Wien, Department für Bildgebende Diagnostik, Clinic for Radiology. To begin with, Dr. Elisabeth Mayrhofer, without whom I would have never acquired the computer tomographic data which is the base of this study; Dr. Sibylle Kneissl, who helped me in gathering basic knowledge about computer-tomographic analysis; Mrs. Sabine Dengg, for her inexhaustible enthusiasm and her efforts in generating the CT-scans.

At the The Museum of Natural History Vienna, Burgring 7, A-1014 Vienna, Department of Zoology I - Mammals, Dr. Barbara Herzig and Mr. Alexander Bibl were my most important source of material concerning *Crocuta crocuta* and *Hyaena hyaena*, for which I am especially grateful.

Many thanks go to Dr. Reinhard Ziegler (Museum am Löwentor, Rosenstein 1, 70191 Stuttgart), who was a very nice host during my short visit to Stuttgart, and who provided me with three of the very precious and rare *Crocuta crocuta spelaea*-skulls for this study. Furthermore for his patience with me despite all the additional questions I had later on. My thanks go also to Mr. Thomas Raathgeber for the photographs of specimen no 6617.

At the Department of Anthropology, University of Vienna, I want to thank Dr. Gerhard Weber who provided the most essential knowledge and techniques for virtual analysis with computer tomographic data. Furthermore for supplying me with a computer for the basal work and the necessary software licenses. Again I want to thank especially Mag. Simon Neubauer, but also Mag. Philip Gunz and Andrea Stadlmayr, for constructive ideas and an open ear for all my worries through the editing process. I know it is hard to have me in the same office!

At the Katharinenhospital, Institut für diagnostische und interventionelle Radiologie, Kriegsbergstraǧe 60, 70174 Stuttgart, Stefan Würstlin MD and Mrs. Yvonne Dinger, who made the CT-scans for specimen no 6617 from the Museum am Löwentor.

And finally Dr. Johann Hohenegger for his help and advice with the interpretation of my statistical analyses.

Glossary

Amira A computer software from Mercury Computer Systems to process computer tomographic data. The version used for this study is Amira 3.1.

Analyze A computer software from the Mayo Foundation to process computer tomographic data. The version used for this study is Analyze 4.0.

anterior view The same as coronal view; A view from the front.

Basion A craniometric point on the skull which lies where the frontal edge of the *foramen magnum* intersects with the median sagittal plain. It is exactly opposite the *Opisthion*.

Bregma A craniometric point on the skull, the Bregma is the crosspoint between the left and right parietal bone and left and right frontal bone.

Bregma cf Because it was not possible to see the bone fissures in the CT-scans, I defined the *Bregma cf* as the point where the left and right arcs of the *pars temporalis* of the frontal bone merge.

coronal view The same as anterior view; A view from the front.

cranial capacity The cranial capacity is the volume of the endocranial cavity. Thus it is a measurement for brain size.

dorsal view The same as transverse view; a view from the top.

$F - Test$ A statistical method that gives the possibility of comparing different sample groups for parameter-influenced differences.

HMH Half maximum height; a method used in computer tomographic survey to generate an average threshold between bone and air for volume measurement of skull cavities.

Inion A craniometric point on the skull which is defined on the median sagittal plain where the two *liniae nuchae superiores* merge, which is very often visible in transverse view as a beak at the most aboral part of the sagittal crest. It is however not the external occipital protuberance, which in hyenasis is more often situated above the Inion.

$Kolmogorov - Smirnov - Test$ A statistical method used to verify if the samples of a group have Gaussian distribution.

lateral view A view from either the left or the right side.

multislicer A modern computer tomograph which is capable of scanning multiple slices at once. Often these devices are also capable of doing real-time scans which means about 25 images per second. That can be used to watch organs (like heart activity) work in real time.

Nasion A craniometric point on the skull which is defined as the crosspoint between the left and right frontal bone and the left and right nasal bone.

Opisthion A craniometric point on the skull which lies where the back edge of the *foramen magnum* intersects with the median sagittal plain. It is exactly opposite the *Basion*.

processus zygomaticus It is an appendix situated above each orbita and marks the rest of the connection of the frontal bone with the zygomatic arch.

Prosthion A craniometric point on the skull which is defined as the point on the median sagittal plain which lies in the exact center between the two I^1.

$radon\ back - transform$ Developed from the original radontransform, this method is used in the image creation process of computer tomographs.

radontransform A mathematical formula through which it is possible to generate the typical CT-images and data-sets. Developed by an Austrian mathematician in the beginning of the 20th century.

raw data Reference to the original data produced by the computer tomograph without processing through the radon back-transform to acquire usable images.

sagittal view The same as lateral or medial view; a view from the side.

sinal cavity This term is used in this study as reference to both, nasal and frontal sinus cavities.

slice A single image out of a computer-tomographic dataset. A complete set is composed of a great number of slices.

Spina nasalis posterior A craniometric point on the skull which is the most aboral point of the secondary palatum along the median sagittal plain.

$spiral - CT$ A modern computer tomograph which is able, in addition to the single-slice-method, to do a spiral analysis of the patient, which results in shorter analysis time and thus lower radiation exposure to the patient.

$t - Test$ A statistical method that gives the possibility of telling if two sample groups belong to the same basic population.

transverse view The same as dorsal view; a view from the top.

ventral view A view from under the specimen.

virtual endocast This term specifies the virtual filling of a cavity. In this study exist sinal virtual endocasts (specifying the filling of the sinal cavity) and endocranial virtual endocasts (specifying the cranial capacity).

voxel A three-dimensional pixel; a pixel is a defined area in a digital image with fixed length and breadth. A voxel adds depth to this information, and thus results in a kind of cube. All computer tomographic datasets are composed of voxels.

List of Figures

List of Tables

Bibliography

Andree, J. (1939). *Der eiszeitliche Mensch in Deutschland und seine Kulturen*. Verlag von Ferdinand Enke, Stuttgart.

Baryshnikov, G. (1999). Chronological and Geographical Variability of Crocuta spelaea (Carnivora, Hyaenidae) from the Pleistocene of Russia. In Haynes, G., Klimovicz, J., and Reumer, J. W. F., editors, *Mammoths and the Mammoth Fauna: Studies of an Extinct Ecosystem*, pages 155–174. Natural History Museum, Rotterdam.

Beyerer, J. and León, F. P. (2002). Die Radontransformation in der digitalen Bildverarbeitung. In *Automatisierungstechnik 50 (2002) 10*. Oldenbourg Verlag, München.

Conroy, G. C. and Vannier, M. W. (1984). Noninvasive three-dimensional computer imaging of matrix-filled fossil skulls by high-resolution computed tomography. *Science*, (226):456–458.

Ehrenberg, K., Sickenberg, O., and Stifft-Gottlieb, A. (1938). *Die Fuchs- oder Teufelslucken bei Eggenburg, Niederdonau*, volume XVII. Verlag der Zoologisch-Botanischen Gesellschaft, Wien.

Elser, T. (2004). *Statistik für die Praxis*. Wiley-VCH Verlag GmbH & Co. KGaA, Weinheim, 1 edition.

Erxleben, J. C. P. (1777). *Systema regni animalis, Classis I, Mammalia*. Lipsiæ.

Esper, J. F. (1774). *Ausführliche Nachricht von neuentdeckten Zoolithen unbekannter vierfüssiger Tiere*. Knorr, Nürnberg.

Fraas, E. (1893). –. *Zeitschrift Deutsche Geologische Gesellschaft*, (45).

Goldfuss, G. A. (1823). V. Ueber den Hölenwolf (Canis spelaeus). In *Osteologische Beiträge zur Kenntniß verschiedener Säugetiere der Vorwelt (Fortsetzung)*, volume 11, pages 451–455.

Heller, F. (1972). Die Zoolithenhöhle bei Burggaillenreuth/Ofr. — 200 Jahre wissenschaftliche Forschung 1771–1971. *Erlanger Forschungen*, 5.

Hofreiter, M., Rabeder, G., Jaenicke-Després, V., Withalm, G., Nagel, D., Paunovic, M., Jambrĕsić, G., and Pääbo, S. (2004). Evidence for reproductive isolation between cave bear populations. *Current Biology*, 14:40–43.

Jánossy, D. (1986). *Pleistocene Vertebrate Faunas of Hungary.* Akadémiai Kiadó, Budapest.

Joeckel, R. M. (1998). Unique Frontal Sinuses in Fossil and Living Hyaenidae (Mammalia, Carnivora): Description and Interpretation. *Journal of Vertebrate Paleontology,* 18(3):627–639.

Kruuk, H. (1972). *The Spotted Hyena: a Study of Predation and Social Behavior.* University of Chicago Press, Chicago.

Kurtén, B. (1956). The status and affinites of hyaena sinensis owen and hyaena ultima matsumoto. *American Museum Novitates,* (1764).

Linnaeus, C. (1758). *Systema Naturae.* Weinheim, Stockholm, 10 edition. http://dz-srv1.sub.uni-goettingen.de/cache/toc/D265100.html.

Markova, A. K., Smirnov, N. G., Kozharinov, A. V., Kazantseva, N. E., Simakova, N., and Kitaev, L. M. (1995). Late pleistocene distribution and diversity of mammals in northern eurasia. *Paleontologia i Evolucio,* 28–29:5–134.

Musil, R. (1980). Ursus spelaeus, der Höhlenbär. *Weimarer Monographien zur Ur- und Frühgeschichte,* I-II.

Musil, R. (1981). Ursus spelaeus, der Höhlenbär. *Weimarer Monographien zur Ur- und Frühgeschichte,* III.

Neischl, A. (1903). *Die Höhlen der fränkischen Schweiz und ihre Bedeutung für die Entstehung der dortigen Täler.* PhD thesis, Erlangen.

Neischl, A. (1904). *Die Höhlen der Fränkischen Schweiz und ihre Bedeutung für die Entstehung der dortigen Täler.* Johann Leonard Schrag, Nürnberg.

Pales, L. and Lambert, C. (1971). *Atlas Ostéologique Mammifères du Quaternaire - Carnivores.* Éditions du Centre National de la Recherche Scientifique, Paris.

Rohland, N., Pollack, J. L., Nagel, D., Beauval, C., Airvaux, J., Pääbo, S., and Hofreiter, M. (2005). The population history of extant and extinct hyenas. *Molecular Biology and Evolution,* 22(12):2435–2443.

Schwenkel, H. (1950). *Das Heimatbuch des Kreises Nürtingen,* volume I. Triltsch.

Sparrmann, A. (1783). *Resa till Goda Hopps-Udden Södra Polkretsern och Omkring Jordklotet samt till Hottentott- och Caffer-landern åren 1772-76.* A.J. Nordströrm, Stockholm.

Stuart, A. J. (1991). Mammalian extinctions in the late Pleistocene of northern Eurasia and North America. *Biological Reviews,* 66:453–562.

Thunberg, C. P. (1820). Beskrifning och teckning på ett nytt species, Hyaena brunnea. *Kongliga Vetenskapsakademiens Handlingar för år*, pages 59–65.

Weber, G. W., Recheis, W., Scholze, T., and Seidler, H. (1998). Virtual Anthropology (VA): Methodical Aspects of Linear and Volume Measurements - First Results. *Coll. Antropol.*, 22(2):575–583.

Wehner, R. and Gehring, W. (1995). *Zoologie.* Georg Thieme Verlag, Stuttgart, New York, 23 edition.

Werdelin, L. and Solounias, N. (1991). *The Hyaenidae: taxonomy, systematics and evolution.* Number 30 in Fossils and Strata. Universitetsforlaget, Oslo.

Wind, J. (1980). X-ray analysis of fossil hominid temporal bones. *Antrop Contemp*, 3:299.

Index